

Contents lists available at ScienceDirect

### Journal of Computational and Applied Mathematics

journal homepage: www.elsevier.com/locate/cam



## Analytic approximations for pricing perpetual American strangle options under constant elasticity of variance model with stochastic volatility

Sun-Yong Choi <sup>a</sup>, Mijin Ha <sup>b</sup>, Sangmin Park <sup>b</sup>, Ji-Hun Yoon <sup>b,c</sup>, <sup>\*</sup>

- <sup>a</sup> Department of Finance and Big Data, Gachon University, Gyeoggi 13120, Republic of Korea
- <sup>b</sup> Department of Mathematics, Pusan National University, Busan 46241, Republic of Korea
- <sup>c</sup> Institute of Mathematical Science, Pusan National University, Busan 46241, Republic of Korea

#### ARTICLE INFO

# Keywords: Perpetual American strangle option Constant elasticity of variance Fast mean reversion Asymptotic analysis Monte-Carlo simulation Call option Pull option Stochastic volatility

#### ABSTRACT

Generally, a perpetual American strangle option is an investment strategy integrating the characteristics of call and put options under an underlying asset with an infinite time horizon. Investors commonly use this trading strategy as they anticipate the underlying asset to fluctuate considerably but are uncertain about an increase or decrease. In this study, we consider the perpetual American strangle options under the Stochastic Volatility Constant Elasticity of Variance (SVCEV) model and examine the approximated option prices and free boundary values using an asymptotic analysis. Moreover, we verify the pricing accuracy of the approximated solutions for perpetual American strangle options under SVCEV by comparing our solutions with the prices derived from Monte Carlo simulations. Finally, we analyze the price sensitivities of the options and free boundaries in terms of several model parameters. Our findings emphasize that the influence of the SV factor on the option price or the optimal exercise boundary is significant for the effective volatility and the elasticity parameter.

#### 1. Introduction

Option pricing theory is pivotal in the mathematical finance field. Particularly, volatility is considered essential in pricing derivatives, dynamic hedging, and portfolio management in financial markets. For instance, the price for foreign exchange (FX) options is commonly quoted in terms of volatility. Moreover, volatility has become a focus of academic research and practical applications because of its importance in the valuation of financial derivatives.

Meanwhile, methods to model volatility have been under study for many years. The Black–Scholes model [1] is one of the most popular models. However, for such a model, significant challenges have arisen in modeling volatility to capture and reflect the accumulated empirical evidence from financial markets. This is because the Black–Scholes model assumes constant implied volatilities, which contradicts empirical findings revealing that the implied volatilities of equity options often exhibit a smile or skew pattern. Two major types of volatility models have been proposed to address the assumptions in the Black–Scholes model, which are unsuitable for real-world financial industries, and to extend it to account for the skew and smile effects: local and Stochastic volatility (SV) models.

Local volatility models have been developed by Dupire [2] and Derman and Kani [3] for the continuous and discrete cases, respectively, which are collectively referred to as non-parametric local volatility models. In these models, volatility relies on the asset

https://doi.org/10.1016/j.cam.2025.117012

Received 22 January 2025; Received in revised form 4 June 2025

Available online 9 August 2025

0377-0427/© 2025 Elsevier B.V. All rights are reserved, including those for text and data mining, AI training, and similar technologies.

<sup>\*</sup> Corresponding author at: Department of Mathematics, Pusan National University, Busan 46241, Republic of Korea. E-mail address: yssci99@pusan.ac.kr (J.-H. Yoon).

price and time, emphasizing the significance of the correlation between changes in the underlying asset price and the randomness of volatility in pricing options. Furthermore, Cox and Ross [4] proposed the constant elasticity of variance (CEV) model as a parametric local volatility model. Tian et al. [5] highlight that the CEV model can generate a U-shaped implied volatility curve, in contrast to the flat curve assumed in the Black–Scholes model. Nevertheless, in the CEV model proposed by Cox and Ross [4], the volatility and the underlying asset price correlate perfectly, which is entirely positive or negative, depending on the elasticity parameter. In contrast, empirical studies, such as that by Ghysels et al. [6], reveal that there is a definite correlation at all times between the volatility and the risky asset price, displaying the time-varying characteristics of volatility.

Regarding SV models, the extraordinary volatility behaviors observed in financial markets, particularly after the 1987 Financial Crash, have highlighted the significance of non-flat implied volatility. Consequently, participants in financial transactions have increasingly focused on models that can predict financial asset movement. Subsequently, the (pure) SV model was proposed to better describe and reflect real-world financial market conditions after recognizing the SV of an underlying asset. The Heston model (cf. Heston [7]) and the fast mean-reverting SV model proposed by Fouque et al. [8] have become representative SV models designed to capture the mean-reversion phenomenon of volatility observed in real markets. Additionally, the Hull and White model [9] modeled the instantaneous variance process as a geometric Brownian motion. The Heston model [7], with volatility driven by a Cox–Ingersoll–Ross(CIR) process, has been widely regarded as one of the most popular stochastic models due to its analytical tractability.

However, local volatility and SV models do not fully capture empirical evidence revealing that the implied volatility of equity options exhibits smile and skew curves simultaneously. Thus, researchers have proposed a hybrid model that combines these two approaches, stressing that these mixed models are designed to leverage the advantages of local and stochastic volatility frameworks. Choi et al. [10] combined the SV and CEV in a multi-factor model – the hybrid stochastic and local volatility model or the Stochastic Volatility Constant Elasticity of Variance (SVCEV) model – to price the European vanilla options and verify the effectiveness of the hybrid model, comparing it with other models. The SVCEV model has been widely used to evaluate various contingent claims. For instance, Kim et al. [11] developed a pricing formula for European vulnerable options using the SVCEV model, while Kim et al. [12] applied the model to implement the pricing of real options. Choi et al. [13] investigated the analytic pricing formulas for timer options based on the SVCEV model. However, Choi et al. [14] used a multiscale hybrid model incorporating fast and slow factors to evaluate an equity-linked annuity under this framework. Furthermore, Choi et al. [15] used the hybrid stochastic and local volatility model to derive an implied volatility formula for corresponding FX options and conducted calibration experiments to analyze the implied volatilities in three FX option markets. Recently, Cao et al. [16] examined the pricing challenge of a variance swap based on a hybrid of the CEV and SV models. Through option calibration, they compared the SVCEV model with the CEV model and the Heston SV model to evaluate their performance in fitting option data.

In recent years, financial markets have grown more complex and advanced; thus, diverse derivative products designed to maximize investor interest have emerged. One of the securities is the strangle option, which is an investment strategy constructed via call and put options with the same expiration date but different strike prices.

This strategy is typically useful for investors who anticipate dramatic fluctuations of the risky asset but cannot predict the direction. Zaevski [17] revealed that such a phenomenon occurs frequently during periods of high volatility, often supported by volatility clustering observed in real financial markets. Furthermore, Chaput and Ederington [18] and Hull [19] observed that the strangle strategy is the best for risk management and volatility trading. Extensive research has focused on applying strangle options to enhance investment returns or efficiently manage risks associated with sharp price movements in volatile markets. Based on these characteristics, extensive research has focused on applying strangle options to enhance investment returns or efficiently manage risks associated with sharp price fluctuations in volatile markets. For example, Fahlenbrach and Sandas [20] analyzed option strategies, including strangles, in the FTSE-100 index market and studied evidence of order flows in volatility-sensitive strategies. Similarly, Kownatzki et al. [21] examined the potential of strangle options for managing event-risk environments from the Standard and Poor's (S&P) 500 index between 2018 and 2020.

In this article, we investigate the pricing of perpetual American strangle options under the SVCEV model. As previously mentioned, the SV and CEV models were incorporated into a multi-factor model called the hybrid stochastic and local volatility model owing to the disadvantage of the SV or CEV model. This model, introduced by Choi et al. [10], captures the leverage effect to better fit the corresponding market and also addresses the hedging instability caused by the CEV model.

Strangle options, particularly when combined with American options, have been the focus of extensive research. These options allow investors to efficiently manage volatile market risks by enabling early exercise at an optimal stopping time before maturity, offering significant advantages. Consequently, studies have explored the pricing and exercise boundaries of American strangle options. For instance, Chiarella and Ziogas [22] studied the American strangle option as a generalization of McKean's free boundary problem [23] for American options, using the Fourier transform technique. Moraux [24] investigate the perpetual American strangles taking advantage of a nonlinear technique, comparing them with option portfolios. Boyarchenko [25] examined the pricing of perpetual American strangles under a jump-diffusion model. In contrast, Ma and Zhang [26] addressed optimal exercise boundaries through numerical methods, introducing a high-order collocation method for pricing. Ha et al. [27] also studied the perpetual American strangle option pricing using the SV model. In addition, Chang and Sheu [28] considered the pricing of perpetual American strangle and straddle options using a jump-diffusion model. Furthermore, Chuang [29] proposed a quasi-analytical approach to carry out the analysis of the perpetual strangles under the early exercise frontier. Nevertheless, no research has been conducted on the pricing of the perpetual American strangle option (PASO) and its optimal exercise boundary using the hybrid SV and local volatility model to our knowledge. Therefore, we have conducted an extensional study on the pricing of PASOs with SVCEV, referred to as PASO-SVCEV.

The primary contributions of this work are outlined as follows:

Establishing the partial differential equation for PASO-SVCEV: We derive a partial differential equation (PDE) for the value of PASO-SVCEV. Due to the complexity of PDE, introduced by stochastic volatility and local volatility (SVCEV), obtaining a closed-form solution for this PDE is nearly impossible. Furthermore, the mathematical problem of American strangle options requires handling two free boundaries. Thus, we apply the technique of the asymptotic analysis provided by Fouque et al. [8] to derive an approximate option pricing formula and determine the approximated early exercise boundary for PASO-SVCEV.

Validating the pricing formula: Using Monte Carlo simulations, we validate the accuracy of the derived option prices. Specifically, we compute the residual, which is the difference between the Monte Carlo price and our approximated option price. The error between the Monte Carlo price and our approximated option price converges to zero as the number of Monte Carlo paths increases, verifying our pricing accuracy.

Analyzing the impact of SV: We conduct a numerical analysis to investigate the influence of SV on the option price and free boundary values under various model parameters, especially elasticity and effective volatility. Our findings highlight the significant impact of SV on PASO-SVCEV. The effect of the SV factor on the option price and optimal exercise boundary becomes more pronounced in terms of elasticity and effective volatility. Additionally, the free boundary for put options is more sensitive to the SV term than that of call options with respect to the correlation between the risky asset and the volatility, market price of risk, volatility, or elasticity.

The rest of this paper is structured as follows. Section 2 outlines the construction of the model dynamics under the underlying asset price and obtains the PDE for PASO-SVCEV. In Section 3, we present the first-order approximation of the option price using asymptotic analysis. Section 4 validates the accuracy of the approximated option prices for PASOSV and examines the sensitivities of SV factors to the option value with respect to the model parameters. Finally, Section 5 concludes with a summary of key findings and remarks.

#### 2. Model formulation

In this section, we first design a stochastic model for the price of the perpetual American strangle option. Let  $S_t$  be the price of the underlying asset with stochastic volatility and constant elasticity of variance, considering dividend rate q. Let  $V_t$  be the volatility of  $S_t$  following an OU process. Then, the dynamics of  $S_t$  and  $V_t$  under market probability measure  $\mathbb{P}$  is described using the following stochastic differential equations (SDEs):

$$\begin{split} \mathrm{d}S_t &= (\mu - q)S_t \mathrm{d}t + f(V_t)S_t^{\theta/2} \mathrm{d}W_t, \\ \mathrm{d}V_t &= \alpha(m - V_t) \mathrm{d}t + \beta \left( \rho \mathrm{d}W_t + \sqrt{1 - \rho^2} \mathrm{d}Z_t \right), \end{split} \tag{2.1}$$

where  $\mu$  denotes the expected return rate, f is a smooth function bounded by positive constants  $c_1$  and  $c_2$ , such that  $0 < c_1 \le f \le c_2 < \infty$  and  $\theta$  is an elasticity parameter. In addition,  $\alpha$  and  $\beta$  are positive constants, m is the long-term mean of  $V_t$ , and  $\rho$  represents the correlation between the standard Brownian motions  $W_t$  and  $Z_t$ , with  $\rho$  satisfying  $-1 \le \rho \le 1$ .

The OU process  $V_t$  is an ergodic process with the mean-reverting property and  $V_t$  is expressed as  $V_t = m + (V_0 - m)e^{at} + \beta \int_0^t e^{-\alpha(t-s)} dZ_s$ . Thus,  $V_t$  follows the normal distribution  $\mathcal{N}(m + (V_0 - m)e^{-at}, u^2(1 - e^{-2at}))$ . As  $t \to \infty$ ,  $V_t$  is independent to  $V_0$ , such that  $V_t \sim \mathcal{N}(m, u^2)$ , where m is the mean and  $u = \frac{\beta}{\sqrt{2\alpha}}$  is the standard deviation of the invariant distribution of  $V_t$ . Suppose

that the mean reversion rate  $\alpha$  is sufficient; in that case,  $V_t$  returns to the mean of its invariant distribution independently of time. Therefore, we consider a sufficiently small parameter  $\epsilon$ , defined as the reciprocal of the mean reversion rate  $\alpha$ .

Option prices are represented as the expected value of discounted payoffs under a risk-neutral measure and the no-arbitrage pricing framework. The model's dynamics (2.1) can be reformulated under the risk-neutral probability measure  $\mathbb{P}^*$  by applying the Girsanov theorem [30].

$$dS_{t} = (r - q)S_{t}dt + f(V_{t})S_{t}^{\theta/2}dW_{t}^{*},$$

$$dV_{t} = \left(\frac{1}{\epsilon}(m - V_{t}) - \frac{u\sqrt{2}}{\sqrt{\epsilon}}\Lambda(V_{t})\right)dt + \frac{u\sqrt{2}}{\epsilon}\left(\rho dW_{t}^{*} + \sqrt{1 - \rho^{2}}dZ_{t}^{*}\right),$$
(2.2)

where r is a risk-free interest rate,  $\Lambda$  is expressed as  $\Lambda(y) = \rho \frac{\mu - r}{f(y)} + \gamma(y) \sqrt{1 - \rho^2}$  for the market price of volatility risk  $\gamma(\cdot)$ , and  $W_t^*$  and  $Z_t^*$  are transformed standard Brownian motions under the measure  $\mathbb{P}^*$ .

The analytic form of the price of American-style options remains to be revealed; however, the pricing formula for perpetual American options is well known. Perpetual options are those with no expiry date, signifying that the holder can exercise the option at any time. The option's value is independent of time and is defined as follows for a given underlying asset price  $S_r = s$ .

$$P(s) = \sup_{\tau \in \Gamma[t,\infty)} \mathbb{E}^* \left[ e^{-r(\tau-t)} h(s) \mathbf{1}_{\{\tau < \infty\}} \mid S_t = s \right],$$

where  $\Gamma[t,\infty)$  denotes the set of stopping times  $\tau$  on  $[t,\infty)$  and determines the execution of the option,  $\mathbb{E}^*[\cdot]$  represents the conditional value under the risk neutrality measure and the payoff function of perpetual American options, denoted by h, represents the following forms, depending on whether the option is a call or put— $(S_t - K)^+$  for a call option and  $(K - S_t)^+$  for a put option. Moreover, the optimal execution boundary of the option is defined as  $\tilde{\tau} = \inf\{t_2 > t_1 : S_{t_2} = s_f\}$ , representing the earliest time that the price  $S_{t_2}$ 

of the underlying asset reaches a boundary  $s_f$ . The price and optimal boundary of the perpetual American option are expressed as follows:

$$P(s) = \left(\frac{s_f}{s}\right)^{\frac{2r}{\sigma^2}} \left(K - s_f\right)$$
 and  $s_f = \frac{K}{1 + \frac{\sigma^2}{\sigma}}$ ,

where K, r, and  $\sigma$  are the strike price of the option, risk-free interest rate, and constant volatility of the underlying asset, respectively. The above pricing formula and optimal boundary correspond to a perpetual American put option under the classical Black–Scholes framework, in which the underlying asset follows a geometric Brownian motion with constant volatility.

This characteristic of options provides favorable conditions for investors and expands the possibilities of their use through different strategies. A typical example is the strangle strategy. A strangle is an option's investment strategy that combines a long put and a long call option with strike prices  $K_p$  and  $K_c$ , respectively, according to Chiarella and Ziogas [22]. Here, the condition  $K_p < K_c$  has to be satisfied. Then, the payoff function is defined as

$$h(s) = (K_n - s)^+ + (s - K_c)^+. (2.3)$$

In addition, under the risk-neutral probability measure  $\mathbb{P}^*$ , the PASO's price, denoted by  $\mathcal{V}(s,v)$ , is written as

$$\mathcal{V}(s,v) = \sup_{\tau \in \Gamma(t,\infty)} \mathbb{E}_{s,v}^* \left[ e^{-r(\tau-t)} h(s) \mathbf{1}_{\{\tau < \infty\}} \right]. \tag{2.4}$$

The entire region  $\mathcal{D} = \{(s,v) \mid 0 < s < \infty, 0 < v < \infty\}$  is where prices are defined and can be represented as the union of two regions— $\mathcal{E}$  and  $\mathcal{C}$ .

$$\mathcal{E} = \{ (s, v) \in \mathcal{D} \mid \mathcal{V}(s, v) = (K_p - s)^+ + (s - K_c)^+ \}$$

$$\mathcal{C} = \{ (s, v) \in \mathcal{D} \mid \mathcal{V}(s, v) > (K_p - s)^+ + (s - K_c)^+ \}$$

Also,  $\mathcal{E}$  is divided into two subregions  $\mathcal{E}^p$  and  $\mathcal{E}^c$  which are described as

$$\mathcal{E}^{p} = \{ (s, v) \in \mathcal{D} \mid \mathcal{V}(s, v) = (K_{p} - s)^{+} > 0 \},$$
  
$$\mathcal{E}^{c} = \{ (s, v) \in \mathcal{D} \mid \mathcal{V}(s, v) = (s - K_{c})^{+} > 0 \}.$$

Two boundary values exist because  $\mathcal{E}$  and  $\mathcal{C}$  are regions with no intersection. Both boundary values— $s_{f,c}$  and  $s_{f,p}$ —can be represented as follows:

$$s_{f,p}(v) = \sup\{s \mid (s,v) \in \mathcal{E}^p\} \quad \text{and} \quad s_{f,c}(v) = \inf\{s \mid (s,v) \in \mathcal{E}^c\},$$

which is called the free boundary of PASO. Therefore, the continuous region C can be redefined as follows:

$$C = \{(s, v) \mid s_{f, p} < s < s_{f, c}\}.$$

Subsequently, we can transform the given optimal stopping time problem (2.4) into the following free boundary problem by applying the methodology of Tao [31],

$$\frac{1}{2}f(v)^{2}s^{\theta}\frac{\partial^{2}V}{\partial s^{2}} + r(s-q)\frac{\partial V}{\partial s} - rV + \frac{\sqrt{2}u}{\sqrt{\epsilon}}\left(\rho f(v)s^{\theta/2}\frac{\partial^{2}V}{\partial s\partial v} - \Lambda(v)\frac{\partial V}{\partial v}\right) + \frac{1}{\epsilon}\left((m-v)\frac{\partial V}{\partial v} + u^{2}\frac{\partial^{2}V}{\partial v^{2}}\right) = 0$$
(2.5)

for  $(s, v) \in (s_{f,p}, s_{f,c}) \times (-\infty, +\infty)$ , together with the four boundary conditions

$$\mathcal{V}(s_{f,p}(v), v) = K_p - s_{f,p}, 
\mathcal{V}(s_{f,c}(v), v) = s_{f,c} - K_c, 
\frac{\partial \mathcal{V}}{\partial s}(s_{f,p}(v), v) = -1, 
\frac{\partial \mathcal{V}}{\partial s}(s_{f,c}(v), v) = 1, 
(2.6)$$

when  $K_c > K_p$ . Here, the first and second equations in (2.6) are matching conditions for the put and call, respectively and the third and fourth equations in (2.6) correspond to the smooth pasting conditions with respect to s. The PDE (2.5) can be described as

$$\left(\tilde{\mathcal{L}}_2 + \frac{1}{\sqrt{\epsilon}}\tilde{\mathcal{L}}_1 + \frac{1}{\epsilon}\tilde{\mathcal{L}}_0\right)\mathcal{V}(s, v) = 0,\tag{2.7}$$

by defining the operators in the following manner:

$$\tilde{\mathcal{L}}_{0} = (m - v)\frac{\partial}{\partial v} + u^{2}\frac{\partial^{2}}{\partial v^{2}},$$

$$\tilde{\mathcal{L}}_{1} = \sqrt{2}\rho u f(v)s^{\theta/2}\frac{\partial^{2}}{\partial s\partial y} - \sqrt{2}u\Lambda(v)\frac{\partial}{\partial v},$$

$$\tilde{\mathcal{L}}_{2} = \frac{1}{2}f^{2}(v)s^{\theta}\frac{\partial^{2}}{\partial v^{2}} + (r - q)s\frac{\partial}{\partial s} - r\mathcal{I},$$
(2.8)

where  $\mathcal{I}$  is an identity operator. We use the following new variables to find  $\mathcal{V}$ , which satisfies the PDE (2.7):

$$x = \ln s$$
,  $x_{f,c} = \ln s_{f,c}$ ,  $x_{f,p} = \ln s_{f,p}$ , and  $Q(x,v) = \mathcal{V}(s,v)$ .

Then, the PDE (2.7) is converted into

$$\left(\mathcal{L}_2 + \frac{1}{\sqrt{\epsilon}}\mathcal{L}_1 + \frac{1}{\epsilon}\mathcal{L}_0\right)Q(x, v) = 0,$$

with the operators

$$\mathcal{L}_{0} = (m - v)\frac{\partial}{\partial v} + u^{2}\frac{\partial^{2}}{\partial v^{2}},$$

$$\mathcal{L}_{1} = \sqrt{2}\rho u f(v)e^{(\theta/2-1)x}\frac{\partial^{2}}{\partial x \partial v} - \sqrt{2}u\Lambda(v)\frac{\partial}{\partial v},$$

$$\mathcal{L}_{2} = \frac{1}{2}f^{2}(v)e^{(\theta-2)x}\frac{\partial^{2}}{\partial x^{2}} + \left(r - q - \frac{1}{2}f^{2}(v)e^{(\theta-2)x}\right)\frac{\partial}{\partial x} - r\mathcal{I}.$$

$$(2.9)$$

Subsequently, the linear complementarity problem with four boundary conditions is obtained as follows:

$$\mathcal{L}^{\epsilon}Q(x,v) = 0, \quad (x,v) \in (x_{f,p}, x_{f,c}) \times (-\infty, +\infty),$$

$$Q(x_{f,p}(v), v) = K_p - e^{x_{f,p}},$$

$$Q(x_{f,c}(v), v) = e^{x_{f,c}} - K_c,$$

$$\frac{\partial Q}{\partial x}(x_{f,p}(v), v) = -e^x,$$

$$\frac{\partial Q}{\partial x}(x_{f,c}(v), v) = e^x,$$
(2.10)

where the differential operator  $\mathcal{L}^{\varepsilon}$  is  $\mathcal{L}^{\varepsilon} = \mathcal{L}_2 + \frac{1}{\sqrt{\varepsilon}}\mathcal{L}_1 + \frac{1}{\varepsilon}\mathcal{L}_0$ .

#### 3. Option price approximation

Based on the work by Fouque et al. [8], when the option price Q(x, v) and free boundaries— $x_{f,p}(v)$  and  $x_{f,c}(v)$ —are asymptotically expanded in terms of the small parameter  $\sqrt{\epsilon}$  for  $0 < \epsilon \ll 1$ , the following formal series expansions can be derived:

$$Q(x,v) = \sum_{n=0}^{\infty} \epsilon^{n/2} Q_n^{\epsilon}(x,v), \quad x_{f,p}(v) = \sum_{n=0}^{\infty} \epsilon^{n/2} p_n^{\epsilon}(v), \quad x_{f,c}(v) = \sum_{n=0}^{\infty} \epsilon^{n/2} c_n^{\epsilon}(v)$$

$$(3.1)$$

Substituting (3.1) into the PDE in (2.10) results in

$$\frac{1}{\epsilon} \mathcal{L}_0 Q_0^{\epsilon} + \frac{1}{\sqrt{\epsilon}} (\mathcal{L}_0 Q_1^{\epsilon} + \mathcal{L}_1 Q_0^{\epsilon}) + (\mathcal{L}_0 Q_2^{\epsilon} + \mathcal{L}_1 Q_1^{\epsilon} + \mathcal{L}_2 Q_0^{\epsilon}) + \sqrt{\epsilon} (\mathcal{L}_0 Q_3^{\epsilon} + \mathcal{L}_1 Q_2^{\epsilon} + \mathcal{L}_2 Q_1^{\epsilon}) = \mathcal{O}(\epsilon)$$

$$(3.2)$$

Furthermore, the matching and smooth pasting conditions in (2.10) can be expanded as follows:

$$\begin{split} Q_0^{\epsilon}(c_0^{\epsilon}(v)) + \sqrt{\epsilon} \left( \frac{\partial Q_0^{\epsilon}}{\partial x} (c_0^{\epsilon}(v)) c_1^{\epsilon}(v) + Q_1^{\epsilon}(c_0^{\epsilon}(v)) \right) &= -K_c + e^{c_0^{\epsilon}(v)} + \sqrt{\epsilon} c_1^{\epsilon}(v) e^{c_0^{\epsilon}(v)} + \mathcal{O}(\epsilon), \\ Q_0^{\epsilon}(p_0^{\epsilon}(v)) + \sqrt{\epsilon} \left( \frac{\partial Q_0^{\epsilon}}{\partial x} (p_0^{\epsilon}(v)) p_1^{\epsilon}(v) + Q_1(p_{0,0}(v)) \right) &= K_p - e^{p_0^{\epsilon}(v)} - \sqrt{\epsilon} p_1^{\epsilon}(v) e^{p_0^{\epsilon}(v)} + \mathcal{O}(\epsilon), \\ \frac{\partial Q_0^{\epsilon}}{\partial x} (c_0^{\epsilon}(v)) + \sqrt{\epsilon} \left( \frac{\partial^2 Q_0^{\epsilon}}{\partial x^2} (c_0^{\epsilon}(v)) c_1^{\epsilon}(v) + \frac{\partial Q_1^{\epsilon}}{\partial x} (c_0^{\epsilon}(v)) \right) &= e^{c_0^{\epsilon}(v)} + \sqrt{\epsilon} c_1^{\epsilon}(v) e^{c_0^{\epsilon}(v)} + \mathcal{O}(\epsilon), \\ \frac{\partial Q_0^{\epsilon}}{\partial x} (p_0^{\epsilon}(v)) + \sqrt{\epsilon} \left( \frac{\partial^2 Q_0^{\epsilon}}{\partial x^2} (p_0^{\epsilon}(v)) p_1^{\epsilon}(v) + \frac{\partial Q_1^{\epsilon}}{\partial x} (p_0^{\epsilon}(v)) \right) &= -e^{p_0^{\epsilon}(v)} - \sqrt{\epsilon} p_1^{\epsilon}(v) e^{p_0^{\epsilon}(v)} + \mathcal{O}(\epsilon). \end{split}$$

According to Section 3.2 of Fouque et al. [8], multiplying Eq. (3.2) by  $\epsilon$  eliminates the diverging term. Thus, inserting the expansion (3.1) into the PDE (3.2) results in the following PDEs:

$$\mathcal{L}_{0}Q_{0}^{\epsilon} = 0, 
\mathcal{L}_{0}Q_{1}^{\epsilon} + \mathcal{L}_{1}Q_{0}^{\epsilon} = 0, 
\mathcal{L}_{0}Q_{2}^{\epsilon} + \mathcal{L}_{1}Q_{1}^{\epsilon} + \mathcal{L}_{2}Q_{0}^{\epsilon} = 0, 
\mathcal{L}_{0}Q_{3}^{\epsilon} + \mathcal{L}_{1}Q_{2}^{\epsilon} + \mathcal{L}_{2}Q_{1}^{\epsilon} = 0,$$
(3.4)

 $Q_0^{\epsilon}$  does not depend on the unobserved variable v because  $\mathcal{L}_0$  only acts on v. Similarly, when the growth conditions are applied to the second PDE in (3.4), the correction term  $Q_1^{\epsilon}$  is consequently independent of v. Thus, the third and fourth equations in (3.4) and the centering condition yield a homogeneous equation

$$\mathcal{L}_{\text{CEV}}Q_0^{\epsilon} = 0,$$
 (3.5)

and 
$$\mathcal{L}_{CFV}Q_1^{\epsilon} = G(x),$$
 (3.6)

respectively. Here, the operator  $\langle \mathcal{L}_2 \rangle \triangleq \mathcal{L}_{\text{CEV}}$  with effective volatility  $\bar{\sigma} = \sqrt{\langle f^2 \rangle}$  is given by

$$\mathcal{L}_{\text{CEV}} = \frac{1}{2}\bar{\sigma}^2(v)e^{(\theta-2)x}\frac{\partial^2}{\partial x^2} + \left(r - q - \frac{1}{2}\bar{\sigma}^2(v)e^{(\theta-2)x}\right)\frac{\partial}{\partial x} - r\mathcal{I},\tag{3.7}$$

and the non-homogeneous term G is given as

$$G(x) = \frac{u\rho}{\sqrt{2}} \langle f\phi' \rangle e^{3(\theta/2-1)x} \left( \frac{\partial^3 Q_{0,0}}{\partial x^3} - 3\frac{\partial^2 Q_{0,0}}{\partial x^2} + \frac{\partial Q_{0,0}}{\partial x} \right) + \frac{u}{\sqrt{2}} \left( \rho \langle f\phi' \rangle \theta e^{-3(\theta/2-1)x} - \langle \Lambda\phi' \rangle e^{(\theta-2)x} \right) \left( \frac{\partial^2 Q_{0,0}}{\partial x^2} - \frac{\partial Q_{0,0}}{\partial x} \right), \quad (3.8)$$

where  $\phi(v)$  is a solution of the Poisson equation  $\mathcal{L}_0\phi=f^2(v)-\langle f^2(v)\rangle$  and  $\langle\cdot\rangle=\int_{-\infty}^\infty \cdot \frac{1}{2\pi}\int_{-\infty}^\xi e^{-\frac{z^2}{2}}\mathrm{d}z$  represents the expectation under the invariant distribution of OU process  $V_t$ .

We present the leading order, correction term prices, and free boundaries in the subsequent subsections. First, we expand  $Q_n^{\epsilon}$ ,  $p_n^{\epsilon}$ , and  $c_n^{\epsilon}$  asymptotically with respect to a small parameter  $\delta = 2 - \theta$  for  $0 < \delta \ll 1$ :

$$Q_n^{\epsilon} = \sum_{k=0}^{\infty} \delta^k Q_{n,k}, \quad p_n^{\epsilon} = \sum_{k=0}^{\infty} \delta^k p_{n,k}, \quad \text{and} \quad c_n^{\epsilon} = \sum_{k=0}^{\infty} \delta^k c_{n,k}.$$
(3.9)

As stated by Choi et al. [10] and Kim et al. [32], observations of data (S&P 500 index) from the equity market demonstrate that the constants elasticity  $\theta < 2$  and  $\theta \approx 2$ . We refer to them and assume that  $\theta = 2 - \delta$  for sufficiently small parameter  $0 < \delta \ll 1$ .

#### 3.1. The zeroth-order approximation price $Q_0^{\epsilon}$

We find the hierarchy of PDEs from the PDE (3.5) and an asymptotic expansion (3.9), as follows:

$$\begin{split} \mathcal{L}_{\mathrm{BS}} Q_{0,0} &= 0, \\ \mathcal{L}_{\mathrm{BS}} Q_{0,1} &= \frac{1}{2} \bar{\sigma}^2 x \left( \frac{\partial^2 Q_{0,0}}{\partial x^2} - \frac{\partial Q_{0,0}}{\partial x} \right), \end{split}$$

...

$$\mathcal{L}_{\mathrm{BS}}Q_{0,k} = \frac{1}{2}\bar{\sigma}^2 \sum_{i=1}^k \frac{(-1)^{i+1}x^i}{i!} \left( \frac{\partial^2 Q_{0,k-i}}{\partial x^2} - \frac{\partial Q_{0,k-i}}{\partial x} \right)$$

where

$$\mathcal{L}_{BS}(\bar{\sigma}) = \frac{1}{2}\bar{\sigma}^2 \frac{\partial^2}{\partial x^2} + \left(r - q - \frac{1}{2}\bar{\sigma}^2\right) \frac{\partial}{\partial x} - r\mathcal{I}. \tag{3.10}$$

This PDE system can be obtained from the PDE (3.5) using the Taylor expansion of  $e^{-\delta x}$  with respect to  $\delta$  and comparing the coefficients for each  $\delta$ -order term. In application, we substitute  $\theta = 2 - \delta$  into PDE (3.5). Then, the PDE (3.5) yields

$$\frac{1}{2}\bar{\sigma}^2 e^{(\theta-2)x} \frac{\partial^2 Q_0^{\epsilon}}{\partial x^2} + \left(r - q - \frac{1}{2}\bar{\sigma}^2 e^{(\theta-2)x}\right) \frac{\partial Q_0^{\epsilon}}{\partial x} - rQ_0^{\epsilon} = 0. \tag{3.11}$$

Using the Taylor expansion of  $e^{\delta x}$ , Eq. (3.11) is expressed as

$$\frac{1}{2}\bar{\sigma}^2 \sum_{k=0}^{\infty} \delta^k \frac{(-1)^k x^k}{k!} \frac{\partial^2}{\partial x^2} \sum_{k=0}^{\infty} \delta^k Q_{0,k} + \left(r - q - \frac{1}{2}\bar{\sigma}^2 \sum_{k=0}^{\infty} \delta^k \frac{(-1)^k x^k}{k!}\right) \frac{\partial}{\partial x} \sum_{k=0}^{\infty} \delta^k Q_{0,k} - r \sum_{k=0}^{\infty} \delta^k Q_{0,k} = 0. \tag{3.12}$$

The coefficients of each  $\delta^k$ -order term  $(k \ge 0)$  in Eq. (3.12) are compared, resulting in the following PDE.

• The zero-order term of  $\delta$ :

$$\frac{1}{2}\bar{\sigma}^2 \frac{\partial^2 Q_{0,0}}{\partial x^2} + \left(r - q - \frac{1}{2}\bar{\sigma}^2\right) \frac{\partial Q_{0,0}}{\partial x} - rQ_{0,0} = 0 \tag{3.13}$$

•  $\delta$ -order term :

$$\frac{1}{2}\bar{\sigma}^2 \frac{\partial^2 Q_{0,1}}{\partial x^2} + \left(r - q - \frac{1}{2}\bar{\sigma}^2\right) \frac{\partial Q_{0,1}}{\partial x} - rQ_{0,1} = \frac{1}{2}\bar{\sigma}^2 x \frac{\partial^2 Q_{0,0}}{\partial x^2} - \frac{1}{2}\bar{\sigma}^2 x \frac{\partial Q_{0,0}}{\partial x}$$
(3.14)

•  $\delta^k$ -order term for k > 1

$$\frac{1}{2}\bar{\sigma}^{2}\frac{\partial^{2}Q_{0,k}}{\partial x^{2}} + \left(r - q - \frac{1}{2}\bar{\sigma}^{2}\right)\frac{\partial Q_{0,k}}{\partial x} - rQ_{0,k} = \frac{1}{2}\bar{\sigma}^{2}\sum_{i=1}^{k}\frac{(-1)^{i+1}x^{i}}{i!}\left(\frac{\partial^{2}Q_{0,k-i}}{\partial x^{2}} - \frac{\partial Q_{0,k-i}}{\partial x}\right)$$
(3.15)

Additionally, the matching and smooth pasting conditions presented in (3.3) can be expressed in an expanded form as follows:

$$\begin{split} Q_{0,0}(c_{0,0}(v)) + \sqrt{\varepsilon} \left( \frac{\partial Q_{0,0}}{\partial x}(c_{0,0}(v))c_{0,1}(v) + Q_{0,1}(c_{0,0}(v)) \right) + \delta \left( \frac{\partial Q_{0,0}}{\partial x}(c_{0,0}(v), y)c_{0,1}(v) + Q_{0,1}(c_{0,0}(v)) \right) \\ &= -K_c + e^{c_{0,0}(v)} + \sqrt{\varepsilon}c_{0,1}(v)e^{c_{0,0}(v)} + \delta c_{0,1}(v)e^{c_{0,0}(v)} + \mathcal{O}(\varepsilon, \delta), \\ Q_{0,0}(p_{0,0}(v)) + \sqrt{\varepsilon} \left( \frac{\partial Q_{0,0}}{\partial x}(p_{0,0}(v))p_{0,1}(v) + Q_{0,1}(p_{0,0}(v)) \right) + \delta \left( \frac{\partial Q_{0,0}}{\partial x}(p_{0,0}(v))p_{0,1}(v) + Q_{0,1}(p_{0,0}(v)) \right) \\ &= K_p - e^{p_{0,0}(v)} - \sqrt{\varepsilon}p_{0,1}(v)e^{p_{0,0}(v)} - \delta p_{0,1}(v)e^{p_{0,0}(v)} - \mathcal{O}(\varepsilon, \delta), \\ \frac{\partial Q_{0,0}}{\partial x}(c_{0,0}(v)) + \sqrt{\varepsilon} \left( \frac{\partial^2 Q_{0,0}}{\partial x^2}(c_{0,0}(v))c_{0,1}(v) + \frac{\partial Q_{0,1}}{\partial x}(c_{0,0}(v)) \right) + \delta \left( \frac{\partial^2 Q_{0,0}}{\partial x^2}(c_{0,0}(v))c_{0,1}(v) + \frac{\partial Q_{0,1}}{\partial x}(c_{0,0}(v)) \right) \\ &= e^{c_{0,0}(v)} + \sqrt{\varepsilon}c_{0,1}(v)e^{c_{0,0}(v)} + \delta c_{0,1}(v)e^{c_{0,0}(v)} + \mathcal{O}(\varepsilon, \delta), \\ \frac{\partial Q_{0,0}}{\partial x}(p_{0,0}(v)) + \sqrt{\varepsilon} \left( \frac{\partial^2 Q_{0,0}}{\partial x^2}(p_{0,0}(v))p_{0,1}(v) + \frac{\partial Q_{0,1}}{\partial x}(p_{0,0}(v)) \right) + \delta \left( \frac{\partial^2 Q_{0,0}}{\partial x^2}(p_{0,0}(v))p_{0,1}(v) + \frac{\partial Q_{0,1}}{\partial x}(p_{0,0}(v)) \right) \\ &= -e^{p_{0,0}(v)} - \sqrt{\varepsilon}p_{0,1}(v)e^{p_{0,0}(v)} - \delta p_{0,1}(v)e^{p_{0,0}(v)} + \mathcal{O}(\varepsilon, \delta). \end{split}$$

As demonstrated in Eqs. (3.13)–(3.15), the solution for the leading order price  $Q_{0,0}$  and the correction price  $Q_{0,k}$  for  $k \ge 1$  is obtained.

**Theorem 3.1.** We consider the value of PASO  $Q_{0,0}(x)$ , which satisfies the following free boundary problem:

$$\mathcal{L}_{\text{BS}}Q_{0,0}(x) = 0 \quad \text{for } x \in (p_{0,0}, c_{0,0})$$

$$Q_{0,0}(p_{0,0}) = K_p - e^{p_{0,0}},$$

$$Q_{0,0}(c_{0,0}) = e^{c_{0,0}} - K_c,$$

$$\frac{dQ_{0,0}}{dx}(p_{0,0}) = -e^{p_{0,0}},$$

$$\frac{dQ_{0,0}}{dx}(c_{0,0}) = e^{c_{0,0}}.$$

$$(3.17)$$

The solution  $Q_{0,0}(x)$  is explicitly represented as the solution to the PDE (3.17), as:

$$Q_{0,0}(x) = \frac{\lambda_1 \lambda_2}{\lambda_1 - \lambda_2} (e^{p_{0,0}} - K_p) \left[ \frac{1}{\lambda_1} e^{\lambda_1 (x - p_{0,0})} - \frac{1}{\lambda_2} e^{\lambda_2 (x - p_{0,0})} \right] + \frac{1}{\lambda_1 - \lambda_2} e^{p_{0,0}} \left[ e^{\lambda_2 (x - p_{0,0})} - e^{\lambda_1 (x - p_{0,0})} \right], \tag{3.18}$$

where  $\lambda_1 > 0$  and  $\lambda_2 < 0$  are two distinct real roots of the quadratic equation:

$$\frac{\bar{\sigma}^2}{2}\lambda^2 + \left(r - q - \frac{\bar{\sigma}^2}{2}\right)\lambda - r = 0. \tag{3.19}$$

Additionally, the optimal exercise boundaries— $p_{0,0}$  and  $c_{0,0}$ —are the solutions to the following system of algebraic equations:

$$\frac{\lambda_{1}\lambda_{2}}{\lambda_{1}-\lambda_{2}}e^{p_{0}}\left[\frac{1}{\lambda_{2}}e^{\lambda_{1}(c_{0,0}-p_{0,0})}-\frac{1}{\lambda_{1}}e^{\lambda_{2}(c_{0,0}-p_{0,0})}\right]+\frac{\lambda_{1}\lambda_{2}}{\lambda_{1}-\lambda_{2}}(e^{p_{0,0}}-K_{p})\left[e^{\lambda_{2}(c_{0,0}-p_{0,0})}-e^{\lambda_{1}(c_{0,0}-p_{0,0})}\right]+e^{c_{0,0}}=0,$$

$$\frac{\lambda_{1}\lambda_{2}}{\lambda_{1}-\lambda_{2}}(e^{p_{0,0}}-K_{p})\left[\frac{1}{\lambda_{1}}e^{\lambda_{1}(c_{0,0}-p_{0,0})}-\frac{1}{\lambda_{2}}e^{\lambda_{2}(c_{0,0}-p_{0,0})}\right]+\frac{e^{p_{0,0}}}{\lambda_{1}-\lambda_{2}}\left[e^{\lambda_{2}(c_{0,0}-p_{0,0})}-e^{\lambda_{1}(c_{0,0}-p_{0,0})}\right]-e^{c_{0,0}}+K_{c}=0.$$

$$(3.20)$$

**Proof.** Ha et al. [27] described the process of solving ODE (3.17). The text methodically guides the reader through solving the equation and dealing with the boundary conditions. It also explains setting up the boundary conditions and the limitations to easily understand the steps needed to obtain the solution.

The following theorems describe the expression for the correction price  $Q_{0,k}$  and correction terms for optimal boundaries  $c_{0,k}$  and  $p_{0,k}$  for  $k \ge 1$  for the zero-order term of  $\epsilon$ .

**Theorem 3.2.** The correction term  $Q_{0,1}$  satisfies the following PDE:

$$\mathcal{L}_{\mathrm{BS}}Q_{0,1} = \frac{1}{2}\bar{\sigma}^2x \left(\frac{\mathrm{d}^2Q_{0,0}}{\mathrm{d}x^2} - \frac{\mathrm{d}Q_{0,0}}{\mathrm{d}x}\right) \quad \text{for } x \in (p_{0,0},c_{0,0}),$$
 
$$\frac{\mathrm{d}Q_{0,0}}{\mathrm{d}x}(c_{0,0})c_{0,1} + Q_{0,1}(c_{0,1}) = c_{0,1}e^{c_{0,0}},$$
 
$$\frac{\mathrm{d}Q_{0,0}}{\mathrm{d}x}(p_{0,0})p_{0,1} + Q_{1,0}(p_{0,0}) = -p_{0,1}e^{p_{0,0}},$$
 
$$\frac{\mathrm{d}^2Q_{0,0}}{\mathrm{d}x^2}(c_{0,0})c_{0,1} + \frac{\mathrm{d}Q_{0,1}}{\mathrm{d}x}(c_{0,1}) = c_{0,1}e^{c_{0,0}},$$
 
$$\frac{\mathrm{d}^2Q_{0,0}}{\mathrm{d}x^2}(p_{0,0})p_{0,1} + \frac{\mathrm{d}Q_{0,1}}{\mathrm{d}x}(p_{0,0}) = -p_{0,1}e^{p_{0,0}}.$$
 
$$(3.21)$$

The solution  $Q_{0,1}(x)$  to problem (3.21) is expressed as

$$Q_{0,1}(x) = C_1 e^{\lambda_1 x} + C_2 e^{\lambda_2 x} + D_1 x e^{\lambda_1 x} + D_2 x e^{\lambda_2 x},$$
(3.22)

where  $\lambda_1 > 0$  and  $\lambda_2 < 0$  are two real roots of the quadratic equation (3.19), and the first-order correction terms for the free boundaries— $c_{0,1}$  and  $p_{0,1}$ —are determined by

$$\begin{split} c_{0,1} &= \frac{1}{d} \left[ (B_{11} + B_{12}\lambda_1) D_1 e^{\lambda_1 c_{0,0}} + (B_{11} + B_{12}\lambda_2) D_2 e^{\lambda_2 c_{0,0}} + (B_{13} + B_{14}\lambda_1) D_1 e^{\lambda_1 p_{0,0}} + (B_{13} + B_{14}\lambda_2) D_2 e^{\lambda_2 p_{0,0}} \right] \\ p_{0,1} &= \frac{1}{d} \left[ (B_{21} + B_{22}\lambda_1) D_1 e^{\lambda_1 c_{0,0}} + (B_{21} + B_{22}\lambda_2) D_2 e^{\lambda_2 c_{0,0}} + (B_{23} + B_{24}\lambda_1) D_1 e^{\lambda_1 p_{0,0}} + (B_{23} + B_{24}\lambda_2) D_2 e^{\lambda_2 p_{0,0}} \right], \end{split}$$

where

$$\begin{split} C_1 &= \frac{1}{d} \left[ (B_{31} + B_{32}\lambda_1) D_1 e^{\lambda_1 c_{0,0}} + (B_{31} + B_{32}\lambda_2) D_2 e^{\lambda_2 c_{0,0}} + (B_{33} + B_{34}\lambda_1) D_1 e^{\lambda_1 p_{0,0}} + (B_{33} + B_{34}\lambda_2) D_2 e^{\lambda_2 p_{0,0}} \right] \\ C_2 &= \frac{1}{d} \left[ (B_{41} + B_{42}\lambda_1) D_1 e^{\lambda_1 c_{0,0}} + (B_{41} + B_{42}\lambda_2) D_2 e^{\lambda_2 c_{0,0}} + (B_{43} + B_{44}\lambda_1) D_1 e^{\lambda_1 p_{0,0}} + (B_{43} + B_{44}\lambda_2) D_2 e^{\lambda_2 p_{0,0}} \right] \\ D_1 &= \frac{2Q_1}{\bar{\sigma}^2 \lambda_1^2 + (2r - \bar{\sigma})\lambda_1 - 2r}, \quad D_2 &= \frac{2Q_2}{\bar{\sigma}^2 \lambda_2^2 + (2r - \bar{\sigma})\lambda_2 - 2r}, \\ Q_1 &= \frac{1}{2} \bar{\sigma}^2 \lambda_1 (\lambda_1 - 1) \frac{\lambda_2 \left( K_p - e^{p_{0,0}} \right) + e^{p_{0,0}}}{(\lambda_2 - \lambda_1) e^{p_{0,0}\lambda_1}}, \quad Q_2 &= \frac{1}{2} \bar{\sigma}^2 \lambda_2 (\lambda_2 - 1) \frac{-\lambda_1 \left( K_p - e^{p_{0,0}} \right) + e^{p_{0,0}}}{(\lambda_2 - \lambda_1) e^{p_{0,0}\lambda_2}}, \\ d &= \left( \frac{\mathrm{d}Q_{1,0}}{\mathrm{d}x} (c_{0,0}) - e^{c_{0,0}} \right) \left( \lambda_1 \lambda_2 \left( \frac{\mathrm{d}Q_{1,0}}{\mathrm{d}x} (p_{0,0}) - e^{p_{0,0}} \right) \left( e^{\lambda_1 c_{0,0} + \lambda_2 p_{0,0}} + e^{\lambda_1 p_{0,0} + \lambda_2 c_{0,0}} \right) \right. \\ &\quad + \left( \frac{\mathrm{d}^2 Q_{1,0}}{\mathrm{d}x^2} (c_{0,0}) - e^{p_{0,0}} \right) \left( \lambda_1 e^{\lambda_1 p_{0,0} + \lambda_2 c_{0,0}} - \lambda_1 e^{\lambda_1 c_{0,0} + \lambda_2 p_{0,0}} \right) \\ &\quad + \left( \frac{\mathrm{d}^2 Q_{1,0}}{\mathrm{d}x^2} (p_{0,0}) - e^{p_{0,0}} \right) \left( a^2 e^{\lambda_1 p_{0,0} + \lambda_2 c_{0,0}} - a^2 e^{\lambda_1 c_{0,0} + \lambda_2 p_{0,0}} \right) \\ &\quad + \left( \frac{\mathrm{d}^2 Q_{1,0}}{\mathrm{d}x^2} (p_{0,0}) - e^{p_{0,0}} \right) \left( e^{\lambda_1 c_{0,0} + \lambda_2 p_{0,0}} - e^{\lambda_1 p_{0,0} + \lambda_2 c_{0,0}} \right) \right). \end{split}$$

In the above,

$$\begin{split} B_{11} &= -\lambda_2 e^{\lambda_2 c_{0,0} + \lambda_1 p_{0,0}} \left( \frac{\mathrm{d}^2 Q_{0,0}}{\mathrm{d} x^2} (p_{0,0}) - \frac{\mathrm{d} Q_{0,0}}{\mathrm{d} x} (p_{0,0}) \right) + e^{\lambda_1 c_{0,0} + \lambda_2 p_{0,0}} \left( \frac{\mathrm{d}^2 Q_{0,0}}{\mathrm{d} x^2} (p_{0,0}) - \lambda_2 \frac{\mathrm{d} Q_{0,0}}{\mathrm{d} x} (p_{0,0}) - \left( \lambda_1 - \lambda_2 \right) e^{p_{0,0}} \right), \\ B_{12} &= e^{\lambda_2 c_{0,0} + \lambda_1 p_{0,0}} \left( \frac{\mathrm{d}^2 Q_{0,0}}{\mathrm{d} x^2} (p_{0,0}) - \frac{\mathrm{d} Q_{0,0}}{\mathrm{d} x} (p_{0,0}) \right) - e^{\lambda_1 c_{0,0} + \lambda_2 p_{0,0}} \left( \frac{\mathrm{d}^2 Q_{0,0}}{\mathrm{d} x^2} (p_{0,0}) - \lambda_2 \frac{\mathrm{d} Q_{0,0}}{\mathrm{d} x} (p_{0,0}) - \left( \lambda_1 - \lambda_2 \right) e^{p_{0,0}} \right), \\ B_{13} &= -e^{(\lambda_1 + \lambda_2) c_{0,0}} \left( \frac{\mathrm{d}^2 Q_{0,0}}{\mathrm{d} x^2} (p_{0,0}) - e^{p_{0,0}} \right) \left( \lambda_1 - \lambda_2 \right), \\ B_{14} &= e^{(\lambda_1 + \lambda_2) c_{0,0}} \left( \frac{\mathrm{d} Q_{0,0}}{\mathrm{d} x} (p_{0,0}) - e^{p_{0,0}} \right) \left( \lambda_1 - \lambda_2 \right), \\ B_{21} &= e^{(\lambda_1 + \lambda_2) p_{0,0}} \left( \frac{\mathrm{d}^2 Q_{0,0}}{\mathrm{d} x} (c_{0,0}) - e^{c_{0,0}} \right) \left( \lambda_1 - \lambda_2 \right), \\ B_{22} &= -e^{(\lambda_1 + \lambda_2) p_{0,0}} \left( \frac{\mathrm{d} Q_{0,0}}{\mathrm{d} x} (c_{0,0}) - e^{c_{0,0}} \right) \left( \lambda_1 - \lambda_2 \right), \end{split}$$

$$\begin{split} B_{23} &= -\lambda_2 e^{\lambda_1 c_{0,0} + \lambda_2 p_{0,0}} \left( \frac{\mathrm{d}^2 Q_{0,0}}{\mathrm{d} x^2} (c_{0,0}) - \frac{\mathrm{d} Q_{0,0}}{\mathrm{d} x} (c_{0,0}) \right) - e^{\lambda_2 c_{0,0} + \lambda_1 p_{0,0}} \left( \frac{\mathrm{d}^2 Q_{0,0}}{\mathrm{d} x} (c_{0,0}) - \lambda_2 \frac{\mathrm{d} Q_{0,0}}{\mathrm{d} x} (c_{0,0}) - \left( \lambda_1 - \lambda_2 \right) e^{c_{0,0}} \right), \\ B_{24} &= -e^{\lambda_1 c_{0,0} + \lambda_2 p_{0,0}} \left( \frac{\mathrm{d}^2 Q_{0,0}}{\mathrm{d} x^2} (c_{0,0}) - \frac{\mathrm{d} Q_{0,0}}{\mathrm{d} x} (c_{0,0}) \right) + e^{\lambda_2 c_{0,0} + \lambda_1 p_{0,0}} \left( \frac{\mathrm{d}^2 Q_{0,0}}{\mathrm{d} x^2} (c_{0,0}) - \lambda_2 \frac{\mathrm{d} Q_{0,0}}{\mathrm{d} x} (c_{0,0}) - \lambda_2 \frac{\mathrm{d} Q_{0,0}}{\mathrm{d} x} (c_{0,0}) - \left( \lambda_1 - \lambda_2 \right) e^{c_{0,0}} \right), \\ B_{31} &= -e^{\lambda_2 p_{0,0}} \left( \frac{\mathrm{d}^2 Q_{0,0}}{\mathrm{d} x^2} (c_{0,0}) - e^{c_{0,0}} \right) \left( \frac{\mathrm{d}^2 Q_{0,0}}{\mathrm{d} x^2} (p_{0,0}) - \lambda_2 \frac{\mathrm{d} Q_{0,0}}{\mathrm{d} x} (p_{0,0}) - \left( \lambda_1 - \lambda_2 \right) e^{p_{0,0}} \right), \\ B_{32} &= e^{\lambda_2 p_{0,0}} \left( \frac{\mathrm{d}^2 Q_{0,0}}{\mathrm{d} x} (c_{0,0}) - e^{c_{0,0}} \right) \left( \frac{\mathrm{d}^2 Q_{0,0}}{\mathrm{d} x^2} (p_{0,0}) - \lambda_2 \frac{\mathrm{d} Q_{0,0}}{\mathrm{d} x} (p_{0,0}) - \left( \lambda_1 - \lambda_2 \right) e^{p_{0,0}} \right), \\ B_{33} &= e^{\lambda_2 c_{0,0}} \left( \frac{\mathrm{d}^2 Q_{0,0}}{\mathrm{d} x^2} (p_{0,0}) - e^{p_{0,0}} \right) \left( \frac{\mathrm{d}^2 Q_{0,0}}{\mathrm{d} x^2} (c_{0,0}) - \lambda_2 \frac{\mathrm{d} Q_{0,0}}{\mathrm{d} x} (c_{0,0}) - \left( \lambda_1 - \lambda_2 \right) e^{c_{0,0}} \right), \\ B_{34} &= -e^{\lambda_1 p_{0,0}} \left( \frac{\mathrm{d}^2 Q_{0,0}}{\mathrm{d} x} (p_{0,0}) - e^{p_{0,0}} \right) \left( \frac{\mathrm{d}^2 Q_{0,0}}{\mathrm{d} x^2} (p_{0,0}) - \lambda_2 \frac{\mathrm{d} Q_{0,0}}{\mathrm{d} x} (p_{0,0}) - \left( \lambda_1 - \lambda_2 \right) e^{c_{0,0}} \right), \\ B_{42} &= -e^{\lambda_1 p_{0,0}} \left( \frac{\mathrm{d}^2 Q_{0,0}}{\mathrm{d} x^2} (c_{0,0}) - e^{c_{0,0}} \right) \left( \frac{\mathrm{d}^2 Q_{0,0}}{\mathrm{d} x^2} (p_{0,0}) - \frac{\mathrm{d} Q_{0,0}}{\mathrm{d} x} (c_{0,0}) \right), \\ B_{43} &= -e^{\lambda_1 c_{0,0}} \left( \frac{\mathrm{d}^2 Q_{0,0}}{\mathrm{d} x} (c_{0,0}) - e^{p_{0,0}} \right) \left( \frac{\mathrm{d}^2 Q_{0,0}}{\mathrm{d} x^2} (c_{0,0}) - \frac{\mathrm{d} Q_{0,0}}{\mathrm{d} x} (c_{0,0}) \right), \\ B_{43} &= -e^{\lambda_1 c_{0,0}} \left( \frac{\mathrm{d}^2 Q_{0,0}}{\mathrm{d} x^2} (p_{0,0}) - e^{p_{0,0}} \right) \left( \frac{\mathrm{d}^2 Q_{0,0}}{\mathrm{d} x^2} (c_{0,0}) - \frac{\mathrm{d} Q_{0,0}}{\mathrm{d} x} (c_{0,0}) \right), \\ B_{44} &= e^{\lambda_1 c_{0,0}} \left( \frac{\mathrm{d}^2 Q_{0,0}}{\mathrm{d} x} (p_{0,0}) - e^{p_{0,0}} \right) \left( \frac{\mathrm{d}^2 Q_{0,0}}{\mathrm{d} x^2} (c_{0,0}) - \frac{\mathrm{d} Q_{0,0}}{\mathrm{d} x} (c_{0,0$$

**Proof.** Theorem 3.1 provides the explicit formula for  $Q_{0,0}(x)$ , and using the chain rule leads to

$$Q_{0,0}(x) = \frac{\lambda_2 \left( K_p - e^{p_{0,0}} \right) + e^{p_{0,0}}}{(\lambda_2 - \lambda_1) e^{p_{0,0}\lambda_1}} e^{\lambda_1 x} + \frac{-\lambda_1 \left( K_p - e^{p_{0,0}} \right) + e^{p_{0,0}}}{(\lambda_2 - \lambda_1) e^{p_{0,0}\lambda_2}} e^{\lambda_2 x}. \tag{3.23}$$

We obtain a non-homogeneous ODE for  $Q_{0,1}(x)$  by substituting (3.23) into the ODE for  $Q_{0,1}$ , given by (3.21):

$$\frac{\bar{\sigma}^2}{2} \frac{\mathrm{d}^2 Q_{0,1}(x)}{\mathrm{d} x^2} + \left( r - q - \frac{\bar{\sigma}^2}{2} \right) \frac{\mathrm{d} Q_{0,1}(x)}{\mathrm{d} x} - r Q_{0,1}(x) = Q_1 x e^{\lambda_1 x} + Q_2 x e^{\lambda_2 x}, \tag{3.24}$$

where  $Q_1$  and  $Q_2$  are

$$Q_1 = \frac{1}{2}\bar{\sigma}^2\lambda_1(\lambda_1-1)\frac{\lambda_2\left(K_p - e^{p_{0,0}}\right) + e^{p_{0,0}}}{(\lambda_2-\lambda_1)e^{p_{0,0}\lambda_1}} \quad \text{and} \quad Q_2 = \frac{1}{2}\bar{\sigma}^2\lambda_2(\lambda_2-1)\frac{-\lambda_1\left(K_p - e^{p_{0,0}}\right) + e^{p_{0,0}}}{(\lambda_2-\lambda_1)e^{p_{0,0}\lambda_2}},$$

respectively.

Furthermore, the solution  $Q_{0,1}$  to (3.24), which is the Cauchy-Euler equation, is obtained as:

$$Q_{0,1}(x) = C_1 e^{\lambda_1 x} + C_2 e^{\lambda_2 x} + \frac{2Q_1}{\bar{\sigma}^2 \lambda_1^2 + (2r - \bar{\sigma})\lambda_1 - 2r} x e^{\lambda_1 x} + \frac{2Q_2}{\bar{\sigma}^2 \lambda_2^2 + (2r - \bar{\sigma})\lambda_2 - 2r} x e^{\lambda_2 x} e^{\lambda_2 x} + \frac{2Q_2}{\bar{\sigma}^2 \lambda_2^2 + (2r - \bar{\sigma})\lambda_2 - 2r} x e^{\lambda_2 x} e^{\lambda_2 x} + \frac{2Q_2}{\bar{\sigma}^2 \lambda_2^2 + (2r - \bar{\sigma})\lambda_2 - 2r} x e^{\lambda_2 x} e^{\lambda_2 x} + \frac{2Q_2}{\bar{\sigma}^2 \lambda_2^2 + (2r - \bar{\sigma})\lambda_2 - 2r} x e^{\lambda_2 x} e^{\lambda_2 x} + \frac{2Q_2}{\bar{\sigma}^2 \lambda_2^2 + (2r - \bar{\sigma})\lambda_2 - 2r} x e^{\lambda_2 x} e^{\lambda_2 x} + \frac{2Q_2}{\bar{\sigma}^2 \lambda_2^2 + (2r - \bar{\sigma})\lambda_2 - 2r} x e^{\lambda_2 x} e^{\lambda_2 x} + \frac{2Q_2}{\bar{\sigma}^2 \lambda_2^2 + (2r - \bar{\sigma})\lambda_2 - 2r} x e^{\lambda_2 x} e^{\lambda_2 x} + \frac{2Q_2}{\bar{\sigma}^2 \lambda_2^2 + (2r - \bar{\sigma})\lambda_2 - 2r} x e^{\lambda_2 x} e^{\lambda_2 x} + \frac{2Q_2}{\bar{\sigma}^2 \lambda_2^2 + (2r - \bar{\sigma})\lambda_2 - 2r} x e^{\lambda_2 x} e$$

for real constants  $C_1$  and  $C_2$ . We examine the  $\sqrt{\epsilon}$ -order terms in (3.3) to derive the conditions required to determine  $Q_{0,1}(x)$ ,  $p_{0,1}$ , and  $c_{0,1}$ :

$$\begin{split} &\frac{\mathrm{d}Q_{0,0}}{\mathrm{d}x}(c_{0,0})c_{0,1} + Q_{0,1}(c_{0,0}) = c_{0,1}e^{c_{0,0}},\\ &\frac{\mathrm{d}Q_{0,0}}{\mathrm{d}x}(p_{0,0})p_{0,1} + Q_{0,1}(p_{0,0}) = p_{0,1}e^{p_{0,0}},\\ &\frac{\mathrm{d}^2Q_{0,0}}{\mathrm{d}x^2}(c_{0,0})c_{0,1} + \frac{\mathrm{d}Q_{0,1}}{\mathrm{d}x}(c_{0,0}) = c_{0,1}e^{c_{0,0}},\\ &\frac{\mathrm{d}^2Q_{0,0}}{\mathrm{d}x^2}(p_{0,0})p_{0,1} + \frac{\mathrm{d}Q_{0,1}}{\mathrm{d}x}(p_{0,0}) = p_{0,1}e^{p_{0,0}}. \end{split}$$

In other words,

$$\left( \frac{\mathrm{d}Q_{0,0}}{\mathrm{d}x} (c_{0,0}) - e^{c_{0,0}} \right) c_{0,1} + C_1 e^{\lambda_1 c_{0,0}} + C_2 e^{\lambda_2 c_{0,0}}$$

$$+ \frac{2Q_1}{\bar{\sigma}^2 \lambda_1^2 + (2r - \bar{\sigma})\lambda_1 - 2r} x e^{\lambda_1 c_{0,0}} + \frac{2Q_2}{\bar{\sigma}^2 \lambda_2^2 + (2r - \bar{\sigma})\lambda_2 - 2r} x e^{\lambda_2 c_{0,0}} = 0,$$

$$\left( \frac{\mathrm{d}^2 Q_{0,0}}{\mathrm{d}x^2} (c_{0,0}) - e^{c_{0,0}} \right) c_{0,1} + C_1 \lambda_1 e^{\lambda_1 c_{0,0}} + C_2 \lambda_2 e^{\lambda_2 c_{0,0}}$$

$$+ \frac{2\lambda_1 Q_1}{\bar{\sigma}^2 \lambda_1^2 + (2r - \bar{\sigma})\lambda_1 - 2r} x e^{\lambda_1 c_{0,0}} + \frac{2\lambda_2 Q_2}{\bar{\sigma}^2 \lambda_2^2 + (2r - \bar{\sigma})\lambda_2 - 2r} x e^{\lambda_2 c_{0,0}} = 0,$$

$$\left( \frac{\mathrm{d}Q_{0,0}}{\mathrm{d}x} (p_{0,0}) - e^{p_{0,0}} \right) p_{0,1} + C_1 e^{\lambda_1 p_{0,0}} + C_2 e^{\lambda_2 p_{0,0}}$$

$$+ \frac{2Q_1}{\bar{\sigma}^2 \lambda_1^2 + (2r - \bar{\sigma})\lambda_1 - 2r} x e^{\lambda_1 p_{0,0}} + \frac{2Q_2}{\bar{\sigma}^2 \lambda_2^2 + (2r - \bar{\sigma})\lambda_2 - 2r} x e^{\lambda_2 p_{0,0}} = 0,$$

$$\left( \frac{\mathrm{d}^2 P_{0,0}}{\bar{\sigma}^2 \lambda_1^2 + (2r - \bar{\sigma})\lambda_1 - 2r} x e^{\lambda_1 p_{0,0}} + C_2 \lambda_2 e^{\lambda_2 p_{0,0}} \right)$$

$$+ \frac{2\lambda_1 Q_1}{\bar{\sigma}^2 \lambda_1^2 + (2r - \bar{\sigma})\lambda_1 - 2r} x e^{\lambda_1 p_{0,0}} + C_2 \lambda_2 e^{\lambda_2 p_{0,0}}$$

$$+ \frac{2\lambda_1 Q_1}{\bar{\sigma}^2 \lambda_1^2 + (2r - \bar{\sigma})\lambda_1 - 2r} x e^{\lambda_1 p_{0,0}} + C_2 \lambda_2 e^{\lambda_2 p_{0,0}}$$

$$+ \frac{2\lambda_1 Q_1}{\bar{\sigma}^2 \lambda_1^2 + (2r - \bar{\sigma})\lambda_1 - 2r} x e^{\lambda_1 p_{0,0}} + C_2 \lambda_2 e^{\lambda_2 p_{0,0}}$$

$$+ \frac{2\lambda_1 Q_1}{\bar{\sigma}^2 \lambda_1^2 + (2r - \bar{\sigma})\lambda_1 - 2r} x e^{\lambda_1 p_{0,0}} + C_2 \lambda_2 e^{\lambda_2 p_{0,0}}$$

$$+ \frac{2\lambda_1 Q_1}{\bar{\sigma}^2 \lambda_1^2 + (2r - \bar{\sigma})\lambda_1 - 2r} x e^{\lambda_1 p_{0,0}} + C_2 \lambda_2 e^{\lambda_2 p_{0,0}}$$

To find the four constants  $C_1$ ,  $C_2$ ,  $c_{0,1}$ , and  $p_{0,1}$ , we reformulate the system of Eqs. (3.25) as the matrix representation  $\mathbf{A}\mathbf{x} = \mathbf{b}$ , where  $\mathbf{A}$  denotes a known  $4 \times 4$  coefficient matrix, and  $\mathbf{b}$  is the column vector of constant terms. That is,

$$\begin{split} \mathbf{A} &= \begin{bmatrix} \frac{\mathrm{d}Q_{0,0}}{\mathrm{d}x}(c_{0,0}) - e^{c_{0,0}} & 0 & e^{\lambda_1 c_{0,0}} & e^{\lambda_2 c_{0,0}} \\ \frac{\mathrm{d}^2Q_{0,0}}{\mathrm{d}x^2}(c_{0,0}) - e^{c_{0,0}} & 0 & \lambda_1 e^{\lambda_1 c_{0,0}} & \lambda_2 e^{\lambda_2 c_{0,0}} \\ 0 & \frac{\mathrm{d}Q_{0,0}}{\mathrm{d}x}(p_{0,0}) - e^{p_{0,0}} & e^{\lambda_1 p_{0,0}} & e^{\lambda_2 p_{0,0}} \\ 0 & \frac{\mathrm{d}^2Q_{0,0}}{\mathrm{d}x^2}(p_{0,0}) - e^{p_{0,0}} & \lambda_1 e^{\lambda_1 p_{0,0}} & \lambda_2 e^{\lambda_2 p_{0,0}} \end{bmatrix}, \\ \mathbf{x} &= \begin{bmatrix} c_{0,1} \\ p_{0,1} \\ C_1 \\ C_2 \end{bmatrix}, \\ \mathbf{b} &= - \begin{bmatrix} \frac{2Q_1}{\bar{\sigma}^2 q_1^2 + (2r - \bar{\sigma})\lambda_1 - 2r} e^{\lambda_1 c_{0,0}} + \frac{2Q_2}{\bar{\sigma}^2 \lambda_2^2 + (2r - \bar{\sigma})\lambda_2 - 2r} e^{\lambda_2 c_{0,0}} \\ \frac{2\lambda_1 Q_1}{\bar{\sigma}^2 \lambda_1^2 + (2r - \bar{\sigma})\lambda_1 - 2r} e^{\lambda_1 p_{0,0}} + \frac{2\lambda_2 Q_2}{\bar{\sigma}^2 \lambda_2^2 + (2r - \bar{\sigma})\lambda_2 - 2r} e^{\lambda_2 p_{0,0}} \\ \frac{2\lambda_1 Q_1}{\bar{\sigma}^2 \lambda_1^2 + (2r - \bar{\sigma})\lambda_1 - 2r} e^{\lambda_1 p_{0,0}} + \frac{2Q_2}{\bar{\sigma}^2 \lambda_2^2 + (2r - \bar{\sigma})\lambda_2 - 2r} e^{\lambda_2 p_{0,0}} \\ \frac{2\lambda_1 Q_1}{\bar{\sigma}^2 \lambda_1^2 + (2r - \bar{\sigma})\lambda_1 - 2r} e^{\lambda_1 p_{0,0}} + \frac{2\lambda_2 Q_2}{\bar{\sigma}^2 \lambda_2^2 + (2r - \bar{\sigma})\lambda_2 - 2r} e^{\lambda_2 p_{0,0}} \end{bmatrix}. \end{split}$$

Note that  $det(A) \neq 0$ , indicating that the inverse of A exists. Consequently, x can be determined by multiplying the matrix equation Ax = b by the inverse of A. Specifically,

$$\begin{bmatrix} c_{0,1} \\ p_{0,1} \\ C_1 \\ C_2 \end{bmatrix} = \frac{1}{d} \begin{bmatrix} B_{ij} \end{bmatrix}_{1 \leq i,j \leq 4} \begin{bmatrix} \frac{2Q_1}{\bar{\sigma}^2 q_1^2 + (2r - \bar{\sigma})\lambda_1 - 2r} e^{\lambda_1 c_{0,0}} + \frac{2Q_2}{\bar{\sigma}^2 \lambda_2^2 + (2r - \bar{\sigma})\lambda_2 - 2r} e^{\lambda_2 c_{0,0}} \\ \frac{2\lambda_1 Q_1}{\bar{\sigma}^2 \lambda_1^2 + (2r - \bar{\sigma})\lambda_1 - 2r} e^{\lambda_1 c_{0,0}} + \frac{2\lambda_2 Q_2}{\bar{\sigma}^2 \lambda_2^2 + (2r - \bar{\sigma})\lambda_2 - 2r} e^{\lambda_2 c_{0,0}} \\ \frac{2Q_1}{\bar{\sigma}^2 \lambda_1^2 + (2r - \bar{\sigma})\lambda_1 - 2r} e^{\lambda_1 p_{0,0}} + \frac{2Q_2}{\bar{\sigma}^2 \lambda_2^2 + (2r - \bar{\sigma})\lambda_2 - 2r} e^{\lambda_2 p_{0,0}} \\ \frac{2\lambda_1 Q_1}{\bar{\sigma}^2 \lambda_1^2 + (2r - \bar{\sigma})\lambda_1 - 2r} e^{\lambda_1 p_{0,0}} + \frac{2\lambda_2 Q_2}{\bar{\sigma}^2 \lambda_2^2 + (2r - \bar{\sigma})\lambda_2 - 2r} e^{\lambda_2 p_{0,0}} \end{bmatrix},$$

where, d is a determinant of **A**. Thus, the results are obtained.  $\square$ 

**Theorem 3.3.** For all k > 1, the correction term  $Q_{0,k}$  satisfies the following ODE system:

$$\mathcal{L}_{\mathrm{BS}}Q_{0,k} = \frac{1}{2}\bar{\sigma}^2 \sum_{i=1}^k \frac{(-1)^{i+1}x^i}{i!} \left( \frac{\mathrm{d}^2 Q_{0,k-i}}{\mathrm{d}x^2} - \frac{\mathrm{d}Q_{0,k-i}}{\mathrm{d}x} \right) \triangleq G_{0,k} \quad \text{for } x \in (p_{0,0}, c_{0,0}),$$

$$\frac{\mathrm{d}Q_{0,k-1}}{\mathrm{d}x} (c_{0,0})c_{0,k} + Q_{0,k}(c_{0,0}) = c_{0,k}e^{c_{0,0}}$$

$$\frac{\mathrm{d}Q_{0,k-1}}{\mathrm{d}x} (p_{0,0})p_{0,k} + Q_{0,k}(p_{0,0}) = -p_{0,k}e^{p_{0,0}}$$

$$\frac{\mathrm{d}^2 Q_{0,k-1}}{\mathrm{d}x^2} (c_{0,0})c_{0,k} + \frac{\mathrm{d}Q_{0,k}}{\mathrm{d}x} (c_{0,0}) = c_{0,k}e^{c_{0,0}}$$

$$\frac{\mathrm{d}^2 Q_{0,k-1}}{\mathrm{d}x^2} (p_{0,0})p_{0,k} + \frac{\mathrm{d}Q_{0,k}}{\mathrm{d}x} (p_{0,0}) = -p_{0,k}e^{p_{0,0}}.$$

$$(3.26)$$

Then, the solution  $Q_{0k}(x)$  to problem (3.26) is expressed as

$$Q_{0,k} = C_5 e^{\lambda_1 x} + C_6 e^{\lambda_2 x} - e^{\lambda_1 x} \int_{\rho_0}^{x} \frac{e^{\lambda_2 z} G_{0,k}}{(\lambda_2 - \lambda_1) e^{(\lambda_1 + \lambda_2) z}} dz + e^{\lambda_2 z} \int_{\rho_0}^{x} \frac{e^{\lambda_1 z} G_{0,k}}{(\lambda_2 - \lambda_1) e^{(\lambda_1 + \lambda_2) z}} dz, \tag{3.27}$$

where  $\lambda_1 > 0$  and  $\lambda_2 < 0$  are two real solutions of Eq. (3.19), and the correction terms for the optimal boundaries— $c_{0,k}$  and  $p_{0,k}$ —are represented by

$$\begin{split} c_{0,k} &= \frac{1}{d} \left[ B_{11} \left( e^{\lambda_1 c_{0,0}} D_3 + e^{\lambda_2 c_{0,0}} D_4 \right) + B_{12} \left( e^{\lambda_1 p_{0,0}} D_3 + e^{\lambda_2 p_{0,0}} D_4 \right) \right. \\ & \left. + B_{13} \left( - e^{\lambda_1 c_{0,0}} \left( \lambda_1 D_3 + \widehat{D}_3 \right) + e^{\lambda_2 c_{0,0}} \left( \lambda_2 D_4 + \widehat{D}_4 \right) \right) + B_{14} \left( e^{\lambda_1 p_{0,0}} \left( - \lambda_1 D_3 + \widetilde{D}_3 \right) + e^{\lambda_2 p_{0,0}} \left( \lambda_2 D_4 + \widetilde{D}_4 \right) \right) \right], \\ p_{0,k} &= \frac{1}{d} \left[ B_{21} \left( e^{\lambda_1 c_{0,0}} D_3 + e^{\lambda_2 c_{0,0}} D_4 \right) + B_{22} \left( e^{\lambda_1 p_{0,0}} D_3 + e^{\lambda_2 p_{0,0}} D_4 \right) \right. \\ & \left. + B_{23} \left( - e^{\lambda_1 c_{0,0}} \left( \lambda_1 D_3 + \widehat{D}_3 \right) + e^{\lambda_2 c_{0,0}} \left( \lambda_2 D_4 + \widehat{D}_4 \right) \right) + B_{24} \left( e^{\lambda_1 p_{0,0}} \left( - \lambda_1 D_3 + \widetilde{D}_3 \right) + e^{\lambda_2 p_{0,0}} \left( \lambda_2 D_4 + \widetilde{D}_4 \right) \right) \right], \end{split}$$

where

$$\begin{split} D_3 &= \int_{\rho_{0,0}}^{c_{0,0}} \frac{e^{\lambda_2 z} G_{0,k}}{(\lambda_2 - \lambda_1) e^{(\lambda_1 + \lambda_2) z}} \mathrm{d}z, \qquad \widehat{D}_3 = \frac{e^{\lambda_2 c_{0,0}} G_{0,k}}{(\lambda_2 - \lambda_1) e^{(\lambda_1 + \lambda_2) c_{0,0}}}, \qquad \widetilde{D}_3 = \frac{e^{\lambda_2 \rho_{0,0}} G_{0,k}}{(\lambda_2 - \lambda_1) e^{(\lambda_1 + \lambda_2) \rho_{0,0}}}, \\ D_4 &= \int_{\rho_{0,0}}^{c_{0,0}} \frac{e^{\lambda_1 z} G_{0,k}}{(\lambda_2 - \lambda_1) e^{(\lambda_1 + \lambda_2) z}} \mathrm{d}z, \qquad \widehat{D}_4 = \frac{e^{\lambda_2 c_{0,0}} G_{0,k}}{(\lambda_2 - \lambda_1) e^{(\lambda_1 + \lambda_2) c_{0,0}}}, \qquad \widetilde{D}_4 = \frac{e^{\lambda_2 \rho_{0,0}} G_{0,k}}{(\lambda_2 - \lambda_1) e^{(\lambda_1 + \lambda_2) \rho_{0,0}}}, \\ C_5 &= \frac{1}{d} \left[ B_{31} \left( e^{\lambda_1 c_{0,0}} D_3 + e^{\lambda_2 c_{0,0}} D_4 \right) + B_{32} \left( e^{\lambda_1 \rho_{0,0}} D_3 + e^{\lambda_2 \rho_{0,0}} D_4 \right) \\ &+ B_{33} \left( -e^{\lambda_1 c_{0,0}} \left( \lambda_1 D_3 + \widehat{D}_3 \right) + e^{\lambda_2 c_{0,0}} \left( \lambda_2 D_4 + \widehat{D}_4 \right) \right) + B_{34} \left( e^{\lambda_1 \rho_{0,0}} \left( -\lambda_1 D_3 + \widetilde{D}_3 \right) + e^{\lambda_2 \rho_{0,0}} \left( \lambda_2 D_4 + \widetilde{D}_4 \right) \right) \right], \\ C_6 &= \frac{1}{d} \left[ B_{41} \left( e^{\lambda_1 c_{0,0}} D_3 + e^{\lambda_2 c_{0,0}} D_4 \right) + B_{42} \left( e^{\lambda_1 \rho_{0,0}} D_3 + e^{\lambda_2 \rho_{0,0}} D_4 \right) \\ &+ B_{43} \left( -e^{\lambda_1 c_{0,0}} \left( \lambda_1 D_3 + \widehat{D}_3 \right) + e^{\lambda_2 c_{0,0}} \left( \lambda_2 D_4 + \widehat{D}_4 \right) \right) + B_{44} \left( e^{\lambda_1 \rho_{0,0}} \left( -\lambda_1 D_3 + \widetilde{D}_3 \right) + e^{\lambda_2 \rho_{0,0}} \left( \lambda_2 D_4 + \widetilde{D}_4 \right) \right) \right]. \end{split}$$

Furthermore, d and  $B_{i,j}$  for  $1 \le i, j \le 4$  are defined in Theorem 3.2.

**Proof.** The procedure of the proof is similar to that of Theorem 3.2. The ODE in Eq. (3.26) is transformed into the Cauchy-Euler form. The sum of the first and second terms in (3.27) constitutes the general solution, and the sum of the last two terms is the specific solution.

#### 3.2. The first-order correction price $Q_1^{\epsilon}$

As outlined in Section 3.1, the hierarchy of PDEs with  $Q_{1,k}$  as solutions can be derived from PDE (3.6) and an asymptotic expansion (3.9). The following is provided to elaborate further: First, the PDE (3.6) is described as

$$\frac{1}{2}\bar{\sigma}^2 e^{-\delta x} \frac{\partial^2 Q_1^{\epsilon}}{\partial x^2} + \left(r - q - \frac{1}{2}\bar{\sigma}^2 e^{-\delta x}\right) \frac{\partial Q_1^{\epsilon}}{\partial x} - rQ_1^{\epsilon} = G(x),\tag{3.28}$$

where the non-homogeneous term G(x) is defined by (3.8). Next, using the Taylor expansion of  $e^{-3\delta/2x}$ ,  $e^{3\delta/2x}$ , and  $e^{-\delta x}$ , Eq. (3.28) is expressed as

$$\frac{1}{2}\bar{\sigma}^{2}\sum_{k=0}^{\infty}\delta^{k}\frac{(-1)^{k}x^{k}}{k!}\frac{\partial^{2}}{\partial x^{2}}\sum_{k=0}^{\infty}\delta^{k}Q_{1,k} + \left(r - q - \frac{1}{2}\bar{\sigma}^{2}\sum_{k=0}^{\infty}\delta^{k}\frac{(-1)^{k}x^{k}}{k!}\right)\frac{\partial}{\partial x}\sum_{k=0}^{\infty}\delta^{k}Q_{1,k} - r\sum_{k=0}^{\infty}\delta^{k}Q_{1,k}$$

$$= \frac{1}{\sqrt{2}}u\rho\langle f\phi'\rangle\sum_{k=0}^{\infty}\delta^{k}\frac{(-3)^{k}x^{k}}{2^{k}k!}\left(\frac{d^{3}Q_{0,0}}{dx^{3}} - 3\frac{d^{2}Q_{0,0}}{dx^{2}} + \frac{dQ_{0,0}}{dx}\right)$$

$$+ \frac{1}{\sqrt{2}}u\left(\rho\langle f\phi'\rangle(2 - \delta)\sum_{k=0}^{\infty}\delta^{k}\frac{3^{k}x^{k}}{2^{k}k!} - \langle A\phi'\rangle\sum_{k=0}^{\infty}\delta^{k}\frac{(-1)^{k}x^{k}}{k!}\right)\left(\frac{d^{2}Q_{0,0}}{dx^{2}} - \frac{dQ_{0,0}}{dx}\right).$$
(3.29)

The coefficients of each  $\delta^k$ -order term ( $k \ge 0$ ) in Eq. (3.29) were compared, resulting in the following PDE being derived.

$$\begin{split} \mathcal{L}_{\mathrm{BS}}Q_{1,0} &= \frac{1}{\sqrt{2}}u\rho\langle f\phi'\rangle \left(\frac{\mathrm{d}^3Q_{0,0}}{\mathrm{d}x^3} - 3\frac{\mathrm{d}^2Q_{0,0}}{\mathrm{d}x^2} + 2\frac{\mathrm{d}Q_{0,0}}{\mathrm{d}x}\right) + \frac{1}{\sqrt{2}}u\left(2\rho\langle f\phi'\rangle - \langle \Lambda\phi'\rangle\right) \left(\frac{\mathrm{d}^2Q_{0,0}}{\mathrm{d}x^2} - \frac{\mathrm{d}Q_{0,0}}{\mathrm{d}x}\right),\\ \mathcal{L}_{\mathrm{BS}}Q_{1,1} &= \frac{1}{2}\bar{\sigma}^2x\frac{\mathrm{d}^2Q_{1,0}}{\mathrm{d}x^2} - \frac{1}{2}\bar{\sigma}^2x\frac{\mathrm{d}Q_{1,0}}{\mathrm{d}x} - \frac{3}{2\sqrt{2}}u\rho\langle f\phi'\rangle x\frac{\mathrm{d}^3Q_{0,0}}{\mathrm{d}x^3} \\ &\quad + \frac{1}{\sqrt{2}}u\left(\frac{15}{2}\rho\langle f\phi'\rangle x - \rho\langle f\phi'\rangle + \langle \Lambda\phi'\rangle x\right)\frac{\mathrm{d}^2Q_{0,0}}{\mathrm{d}x^2} - \frac{1}{\sqrt{2}}u\left(\frac{9}{2}\rho\langle f\phi'\rangle x - \rho\langle f\phi'\rangle + \langle \Lambda\phi'\rangle x\right)\frac{\mathrm{d}Q_{0,0}}{\mathrm{d}x}, \end{split}$$

...

$$\begin{split} \mathcal{L}_{\mathrm{BS}}Q_{1,k} &= \frac{1}{2}\bar{\sigma}^2 \sum_{i=1}^k \frac{(-1)^{i+1} x^i}{i!} \left( \frac{\partial^2 Q_{1,k-i}}{\partial x^2} - \frac{\partial Q_{1,k-i}}{\partial x} \right) + \frac{1}{\sqrt{2}} u \rho \langle f \phi' \rangle \frac{(-3)^k x^k}{2^k k!} \frac{\mathrm{d}^3 Q_{0,0}}{\mathrm{d} x^3} \\ &\quad + \frac{1}{\sqrt{2}} u \left( \rho \langle f \phi' \rangle \frac{(-3)^{k+1} x^k}{2^k k!} + \rho \langle f \phi' \rangle \frac{3^k x^k}{2^{k-1} k!} - \rho \langle f \phi' \rangle \frac{3^{k-1} x^{k-1}}{2^{k-1} (k-1)!} - \langle \Lambda \phi' \rangle \frac{(-1)^k x^k}{k!} \right) \frac{\mathrm{d}^2 Q_{0,0}}{\mathrm{d} x^2} \\ &\quad - \frac{1}{\sqrt{2}} u \left( -\rho \langle f \phi' \rangle \frac{(-3)^k x^k}{2^k k!} + \rho \langle f \phi' \rangle \frac{3^k x^k}{2^{k-1} k!} - \rho \langle f \phi' \rangle \frac{3^{k-1} x^{k-1}}{2^{k-1} (k-1)!} - \langle \Lambda \phi' \rangle \frac{(-1)^k x^k}{k!} \right) \frac{\mathrm{d} Q_{0,0}}{\mathrm{d} x}, \end{split}$$

where  $\mathcal{L}_{BS}$  is defined by (3.10).

Furthermore, the matching and smooth pasting conditions in (3.3) can be expressed in their expanded form as:

$$\begin{split} Q_{1,0}(c_{0,0}(v)) + \sqrt{\varepsilon} \left( \frac{\mathrm{d}Q_{1,0}}{\mathrm{d}x}(c_{0,0}(v))c_{1,0}(v) + Q_{1,0}(c_{0,0}(v)) \right) + \delta \left( \frac{\mathrm{d}Q_{1,0}}{\mathrm{d}x}(c_{0,0}(v),y)c_{1,0}(v) + Q_{1,1}(c_{0,0}(v)) \right) \\ &= -K_c + e^{c_{0,0}(v)} + \sqrt{\varepsilon}c_{1,0}(v)e^{c_{0,0}(v)} + \delta c_{1,0}(v)e^{c_{0,0}(v)} + \mathcal{O}(\varepsilon,\delta), \\ Q_{1,0}(p_{0,0}(v)) + \sqrt{\varepsilon} \left( \frac{\mathrm{d}Q_{1,0}}{\mathrm{d}x}(p_{0,0}(v))p_{1,0}(v) + Q_{1,0}(p_{0,0}(v)) \right) + \delta \left( \frac{\mathrm{d}Q_{1,0}}{\mathrm{d}x}(p_{0,0}(v),y)p_{1,1}(v) + Q_{1,1}(p_{0,0}(v)) \right) \\ &= K_p - e^{p_{0,0}(v)} - \sqrt{\varepsilon}Q_{1,0}(v)e^{p_{0,0}(v)} - \delta p_{1,1}(v)e^{p_{0,0}(v)} - \mathcal{O}(\varepsilon,\delta), \\ \frac{\mathrm{d}Q_{1,0}}{\mathrm{d}x}(c_{0,0}(v)) + \sqrt{\varepsilon} \left( \frac{\mathrm{d}^2Q_{1,0}}{\mathrm{d}x^2}(c_{0,0}(v))c_{1,0}(v) + \frac{\mathrm{d}Q_{1,0}}{\mathrm{d}x}(c_{0,0}(v)) \right) + \delta \left( \frac{\mathrm{d}^2Q_{1,0}}{\mathrm{d}x^2}(c_{0,0}(v))c_{1,0}(v) + \frac{\mathrm{d}Q_{1,1}}{\mathrm{d}x}(c_{0,0}(v)) \right) \\ &= e^{c_{0,0}(v)} + \sqrt{\varepsilon}c_{1,0}(v)e^{c_{0,0}(v)} + \delta c_{1,0}(v)e^{c_{0,0}(v)} + \mathcal{O}(\varepsilon,\delta), \\ \frac{\mathrm{d}Q_{1,0}}{\mathrm{d}x}(p_{0,0}(v)) + \sqrt{\varepsilon} \left( \frac{\mathrm{d}^2Q_{1,0}}{\mathrm{d}x^2}(p_{0,0}(v))p_{1,0}(v) + \frac{\mathrm{d}Q_{1,0}}{\mathrm{d}x}(p_{0,0}(v)) \right) + \delta \left( \frac{\mathrm{d}^2Q_{1,0}}{\mathrm{d}x^2}(p_{0,0}(v))p_{1,1}(v) + \frac{\mathrm{d}Q_{1,1}}{\mathrm{d}x}(p_{0,0}(v)) \right) \\ &= -e^{p_{0,0}(v)} - \sqrt{\varepsilon}p_{1,0}(v)e^{p_{0,0}(v)} - \delta p_{1,1}(v)e^{p_{0,0}(v)} + \mathcal{O}(\varepsilon,\delta). \end{split}$$

The following theorems describe the expression for the correction price  $Q_{1,k}$  and correction terms for optimal boundaries— $c_{1,k}$  and  $p_{1,k}$ —for  $k \ge 1$  for the first-order term of  $\epsilon$ .

**Theorem 3.4.** The correction term  $Q_{1,0}$  satisfies the following ODE:

$$\mathcal{L}_{\text{BS}}Q_{1,0} = V_3 \frac{\mathrm{d}^3 Q_{0,0}}{\mathrm{d}x^3} + (V_2 - 3V_3) \frac{\mathrm{d}^2 Q_{0,0}}{\mathrm{d}x^2} + (2V_3 - V_2) \frac{\mathrm{d}Q_{0,0}}{\mathrm{d}x} \quad \text{for } x \in (p_{0,0}, c_{0,0}),$$

$$\frac{\mathrm{d}Q_{1,0}}{\mathrm{d}x}(c_{0,0})c_{1,0} + Q_{1,0}(c_{0,0}) = c_{1,0}e^{c_{0,0}},$$

$$\frac{\mathrm{d}Q_{1,0}}{\mathrm{d}x}(p_{0,0})p_{1,0} + Q_{1,0}(p_{0,0}) = -p_{1,0}e^{p_{0,0}},$$

$$\frac{\mathrm{d}^2 Q_{1,0}}{\mathrm{d}x^2}(c_{0,0})c_{1,0} + \frac{\mathrm{d}Q_{1,0}}{\mathrm{d}x}(c_{0,0}) = c_{1,0}e^{c_{0,0}}$$

$$\frac{\mathrm{d}^2 Q_{1,0}}{\mathrm{d}x^2}(p_{0,0})p_{1,0} + \frac{\mathrm{d}Q_{1,0}}{\mathrm{d}x}(p_{0,0}) = -p_{1,0}e^{p_{0,0}}.$$

$$(3.31)$$

where,  $V_2 = \sqrt{2}\rho u \langle f(y)\phi'(y)\rangle - \frac{\sqrt{2}}{2}u \langle \Lambda(y)\phi'(y)\rangle$  and  $V_3 = \frac{\sqrt{2}}{2}\rho u \langle f(y)\phi'(y)\rangle$ . The solution  $Q_{1,0}(x)$  to problem (3.31) is expressed as

$$Q_{1,0}(x) = C_5 e^{\lambda_1 x} + C_6 e^{\lambda_2 x} + D_5 e^{\lambda_1 x} + D_6 e^{\lambda_2 x}, \tag{3.32}$$

and the first-order correction terms for the free boundaries— $c_{1,0}$  and  $p_{1,0}$ —are determined by

$$\begin{split} c_{1,0} &= \frac{1}{d} \left[ (B_{11} + B_{12}\lambda_1) D_5 e^{\lambda_1 c_{0,0}} + (B_{11} + B_{12}\lambda_2) D_6 e^{\lambda_2 c_{0,0}} + (B_{13} + B_{14}\lambda_1) D_5 e^{\lambda_1 p_{0,0}} + (B_{13} + B_{14}\lambda_2) D_6 e^{\lambda_2 p_{0,0}} \right], \\ p_{1,0} &= \frac{1}{d} \left[ (B_{21} + B_{22}\lambda_1) D_5 e^{\lambda_1 c_{0,0}} + (B_{21} + B_{22}\lambda_2) D_6 e^{\lambda_2 c_{0,0}} + (B_{23} + B_{24}\lambda_1) D_5 e^{\lambda_1 p_{0,0}} + (B_{23} + B_{24}\lambda_2) D_6 e^{\lambda_2 p_{0,0}} \right], \end{split}$$

where

$$\begin{split} C_5 &= \frac{1}{d} \left[ (B_{31} + B_{32}\lambda_1) D_5 e^{\lambda_1 c_{0,0}} + (B_{31} + B_{32}\lambda_2) D_6 e^{\lambda_2 c_{0,0}} + (B_{33} + B_{34}\lambda_1) D_5 e^{\lambda_1 p_{0,0}} + (B_{33} + B_{34}\lambda_2) D_6 e^{\lambda_2 p_{0,0}} \right], \\ C_6 &= \frac{1}{d} \left[ (B_{41} + B_{42}\lambda_1) D_5 e^{\lambda_1 c_{0,0}} + (B_{41} + B_{42}\lambda_2) D_6 e^{\lambda_2 c_{0,0}} + (B_{43} + B_{44}\lambda_1) D_5 e^{\lambda_1 p_{0,0}} + (B_{43} + B_{44}\lambda_2) D_6 e^{\lambda_2 p_{0,0}} \right], \\ D_5 &= \frac{2Q_5}{\bar{\sigma}^2 \lambda_1^2 + (2r - \bar{\sigma})\lambda_1 - 2r}, \quad D_6 &= \frac{2Q_6}{\bar{\sigma}^2 \lambda_2^2 + (2r - \bar{\sigma})\lambda_2 - 2r}, \\ Q_5 &= \left( V_3 \lambda_1^2 + (V_2 - 3V_3)\lambda_1 + 2V_3 - V_2 \right) \frac{\lambda_1 \left( \lambda_2 \left( K_p - e^{p_{0,0}} \right) + e^{p_{0,0}} \right)}{(\lambda_2 - \lambda_1) e^{p_{0,0}\lambda_1}}, \\ Q_6 &= \left( V_3 \lambda_2^2 + (V_2 - 3V_3)\lambda_2 + 2V_3 - V_2 \right) \frac{\lambda_2 \left( -\lambda_1 \left( K_p - e^{p_{0,0}} \right) + e^{p_{0,0}} \right)}{(\lambda_2 - \lambda_1) e^{p_{0,0}\lambda_2}}. \end{split}$$

In addition, d and  $B_{i,j}$  for  $1 \le i, j \le 4$  are defined in Theorem 3.2.

**Proof.** We can derive the solution of the ODE system (3.31) by following a similar stepwise calculation as outlined in Theorem 3.2, providing a detailed framework for obtaining analytical solutions under comparable conditions.

**Theorem 3.5.** The correction term  $Q_{1,1}$  satisfies the following ODE system:

$$\mathcal{L}_{BS}Q_{1,1} = G_{1,1} \quad \text{for } x \in (p_{0,0}, c_{0,0}),$$

$$\frac{dQ_{1,0}}{dx}(c_{0,0})c_{1,1} + Q_{1,1}(c_{0,0}) = c_{1,1}e^{c_{0,0}}$$

$$\frac{dQ_{1,0}}{dx}(p_{0,0})p_{1,1} + Q_{1,1}(p_{0,0}) = -p_{1,1}e^{p_{0,0}}$$

$$\frac{d^2Q_{1,0}}{dx^2}(c_{0,0})c_{1,1} + \frac{dQ_{1,1}}{dx}(c_{0,0}) = c_{1,1}e^{c_{0,0}}$$

$$\frac{d^2Q_{1,0}}{dx^2}(p_{0,0})p_{1,1} + \frac{dQ_{1,1}}{dx}(p_{0,0}) = -p_{1,1}e^{p_{0,0}}.$$

$$(3.33)$$

Where, the non-homogeneous term  $G_{1,1}$  represented by

$$G_{1,1} = \frac{1}{2} \bar{\sigma}^2 x \left( \frac{d^2 Q_{1,0}}{dx^2} - \frac{dQ_{1,0}}{dx} \right) - \frac{3\sqrt{2}}{4} \rho u \langle f(y)\phi'(y) \rangle x \frac{d^3 Q_{0,0}}{dx^3}$$

$$+ \frac{1}{\sqrt{2}} u \left( \frac{15}{2} \rho \langle f\phi' \rangle x - \rho \langle f\phi' \rangle + \langle \Lambda\phi' \rangle x \right) \frac{d^2 Q_{0,0}}{dx^2} - \frac{1}{\sqrt{2}} u \left( \frac{9}{2} \rho \langle f\phi' \rangle x - \rho \langle f\phi' \rangle + \langle \Lambda\phi' \rangle x \right) \frac{dQ_{0,0}}{dx}.$$
(3.34)

The solution  $Q_{1,1}(x)$  to problem (3.33) is expressed as

$$Q_{1,1} = C_7 e^{\lambda_1 x} + C_8 e^{\lambda_2 x} - e^{\lambda_1 x} \int_{\rho_{0,0}}^{x} \frac{e^{\lambda_2 z} G_{1,1}}{(\lambda_2 - \lambda_1) e^{(\lambda_1 + \lambda_2) z}} dz + e^{\lambda_2 x} \int_{\rho_{0,0}}^{x} \frac{e^{\lambda_1 z} G_{1,1}}{(\lambda_2 - \lambda_1) e^{(\lambda_1 + \lambda_2) z}} dz, \tag{3.35}$$

where  $\lambda_1 > 0$  and  $\lambda_2 < 0$  are two real roots of the quadratic equation (3.19). Moreover, the correction terms for the optimal boundaries  $c_{1,1}$  and  $p_{1,1}$  are determined by

$$\begin{split} c_{1,1} &= \frac{1}{d} \left[ B_{11} \left( e^{\lambda_1 c_{0,0}} D_7 + e^{\lambda_2 c_{0,0}} D_8 \right) + B_{12} \left( e^{\lambda_1 p_{0,0}} D_7 + e^{\lambda_2 p_{0,0}} D_8 \right) \right. \\ &\quad \left. + B_{13} \left( - e^{\lambda_1 c_{0,0}} \left( \lambda_1 D_7 + \widehat{D}_7 \right) + e^{\lambda_2 c_{0,0}} \left( \lambda_2 D_8 + \widehat{D}_8 \right) \right) + B_{14} \left( e^{\lambda_1 p_{0,0}} \left( -\lambda_1 D_7 + \widetilde{D}_7 \right) + e^{\lambda_2 p_{0,0}} \left( \lambda_2 D_8 + \widetilde{D}_8 \right) \right) \right], \\ p_{1,1} &= \frac{1}{d} \left[ B_{21} \left( e^{\lambda_1 c_{0,0}} D_7 + e^{\lambda_2 c_{0,0}} D_8 \right) + B_{22} \left( e^{\lambda_1 p_{0,0}} D_7 + e^{\lambda_2 p_{0,0}} D_8 \right) \right. \\ &\quad \left. + B_{23} \left( - e^{\lambda_1 c_{0,0}} \left( \lambda_1 D_7 + \widehat{D}_7 \right) + e^{\lambda_2 c_{0,0}} \left( \lambda_2 D_8 + \widehat{D}_8 \right) \right) \right], \end{split}$$

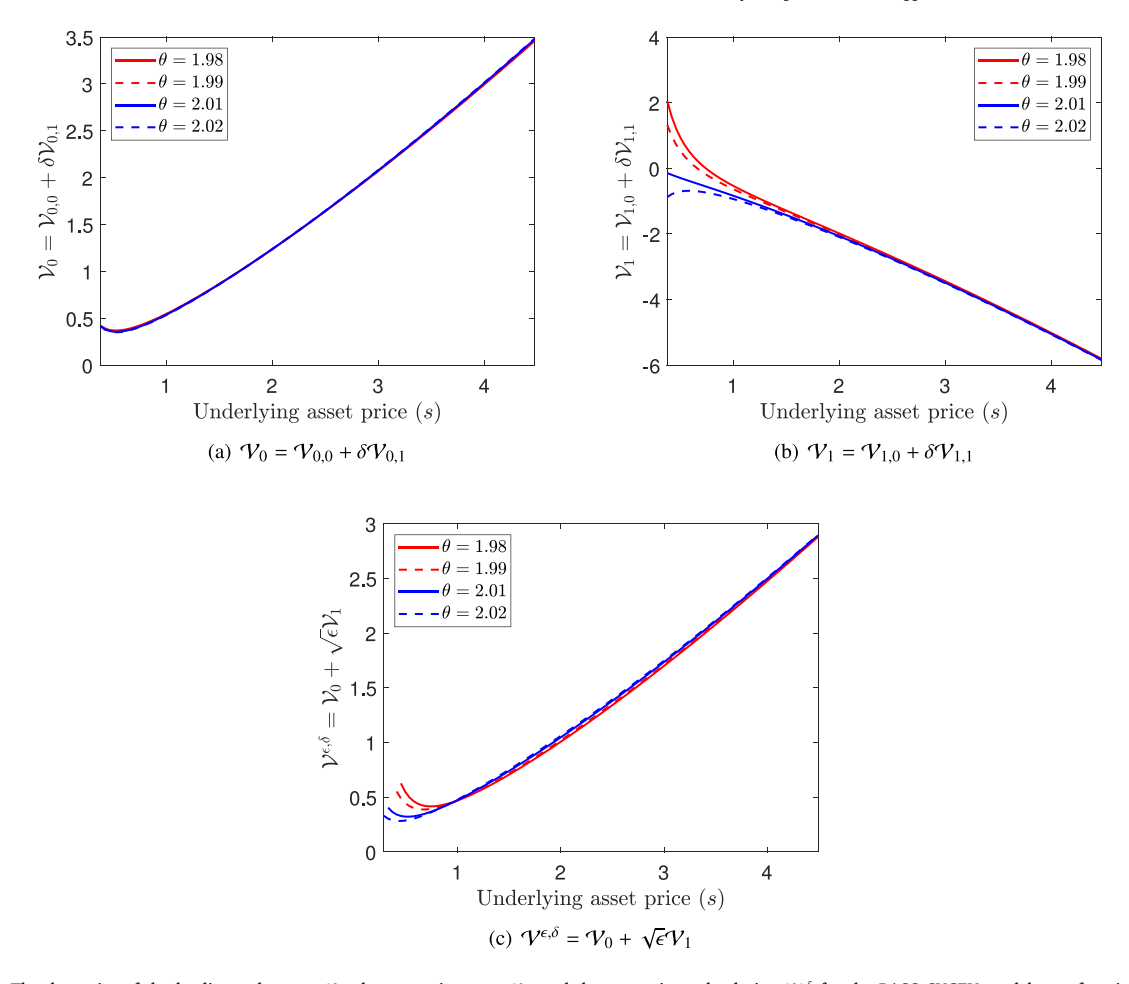


Fig. 1. The dynamics of the leading-order term  $V_0$ , the correction term  $V_1$ , and the approximated solution  $V^{e,\delta}$  for the PASO-SVCEV model as a function of the underlying asset price. The red solid line, red dashed line, blue solid line, and blue dashed line correspond to elasticity values  $\theta = 1.98$ , 1.99, 2.01, and 2.02, respectively.

Notes: The parameters used for this figure are: r = 0.03, q = 0.01,  $K_{\rho} = 0.8$ ,  $K_{c} = 1.0$ ,  $\bar{\sigma} = 0.15$ ,  $\epsilon = 0.001$ ,  $\rho = -0.2$ , m = -1.8594, u = 0.5,  $\langle f(v)\phi'(v)\rangle = 0.1$ , and  $\langle A(v)\phi'(v)\rangle = 0.8266$ .

where

$$\begin{split} D_7 &= \int_{\rho_{0,0}}^{c_{0,0}} \frac{e^{\lambda_2 z} G_{1,1}}{(\lambda_2 - \lambda_1) e^{(\lambda_1 + \lambda_2) z}} \mathrm{d}z, \qquad \widehat{D}_7 = \frac{e^{\lambda_2 c_{0,0}} G_{1,1}}{(\lambda_2 - \lambda_1) e^{(\lambda_1 + \lambda_2) c_{0,0}}}, \qquad \widetilde{D}_7 = \frac{e^{\lambda_2 \rho_{0,0}} G_{1,1}}{(\lambda_2 - \lambda_1) e^{(\lambda_1 + \lambda_2) \rho_{0,0}}}, \\ D_8 &= \int_{\rho_{0,0}}^{c_{0,0}} \frac{e^{\lambda_1 z} G_{1,1}}{(\lambda_2 - \lambda_1) e^{(\lambda_1 + \lambda_2) z}} \mathrm{d}z, \qquad \widehat{D}_8 = \frac{e^{\lambda_2 c_{0,0}} G_{1,1}}{(\lambda_2 - \lambda_1) e^{(\lambda_1 + \lambda_2) c_{0,0}}}, \qquad \widetilde{D}_8 = \frac{e^{\lambda_2 \rho_{0,0}} G_{1,1}}{(\lambda_2 - \lambda_1) e^{(\lambda_1 + \lambda_2) \rho_{0,0}}}, \\ C_7 &= \frac{1}{d} \left[ B_{31} \left( e^{\lambda_1 c_{0,0}} D_7 + e^{\lambda_2 c_{0,0}} D_8 \right) + B_{32} \left( e^{\lambda_1 \rho_{0,0}} D_7 + e^{\lambda_2 \rho_{0,0}} D_8 \right) \right. \\ &\quad \left. + B_{33} \left( -e^{\lambda_1 c_{0,0}} \left( \lambda_1 D_7 + \widehat{D}_7 \right) + e^{\lambda_2 c_{0,0}} \left( \lambda_2 D_8 + \widehat{D}_8 \right) \right) + B_{34} \left( e^{\lambda_1 \rho_{0,0}} \left( -\lambda_1 D_7 + \widetilde{D}_7 \right) + e^{\lambda_2 \rho_{0,0}} \left( \lambda_2 D_8 + \widetilde{D}_8 \right) \right) \right], \\ C_8 &= \frac{1}{d} \left[ B_{41} \left( e^{\lambda_1 c_{0,0}} D_7 + e^{\lambda_2 c_{0,0}} D_8 \right) + B_{42} \left( e^{\lambda_1 \rho_{0,0}} D_7 + e^{\lambda_2 \rho_{0,0}} D_8 \right) \right. \\ &\quad \left. + B_{43} \left( -e^{\lambda_1 c_{0,0}} \left( \lambda_1 D_7 + \widehat{D}_7 \right) + e^{\lambda_2 c_{0,0}} \left( \lambda_2 D_8 + \widehat{D}_8 \right) \right) + B_{44} \left( e^{\lambda_1 \rho_{0,0}} \left( -\lambda_1 D_7 + \widetilde{D}_7 \right) + e^{\lambda_2 \rho_{0,0}} \left( \lambda_2 D_8 + \widetilde{D}_8 \right) \right) \right]. \end{split}$$

Also, d and  $B_{i,j}$  for  $1 \le i, j \le 4$  are defined in Theorem 3.2.

**Proof.** The proof follows a process similar to that of Theorem 3.2. The ODE presented in Eq. (3.33) is reformulated into the Cauchy-Euler equation. The general solution is derived from the sum of the first two terms in (3.35), while the particular solution is represented by the sum of the last two terms.  $\square$ 

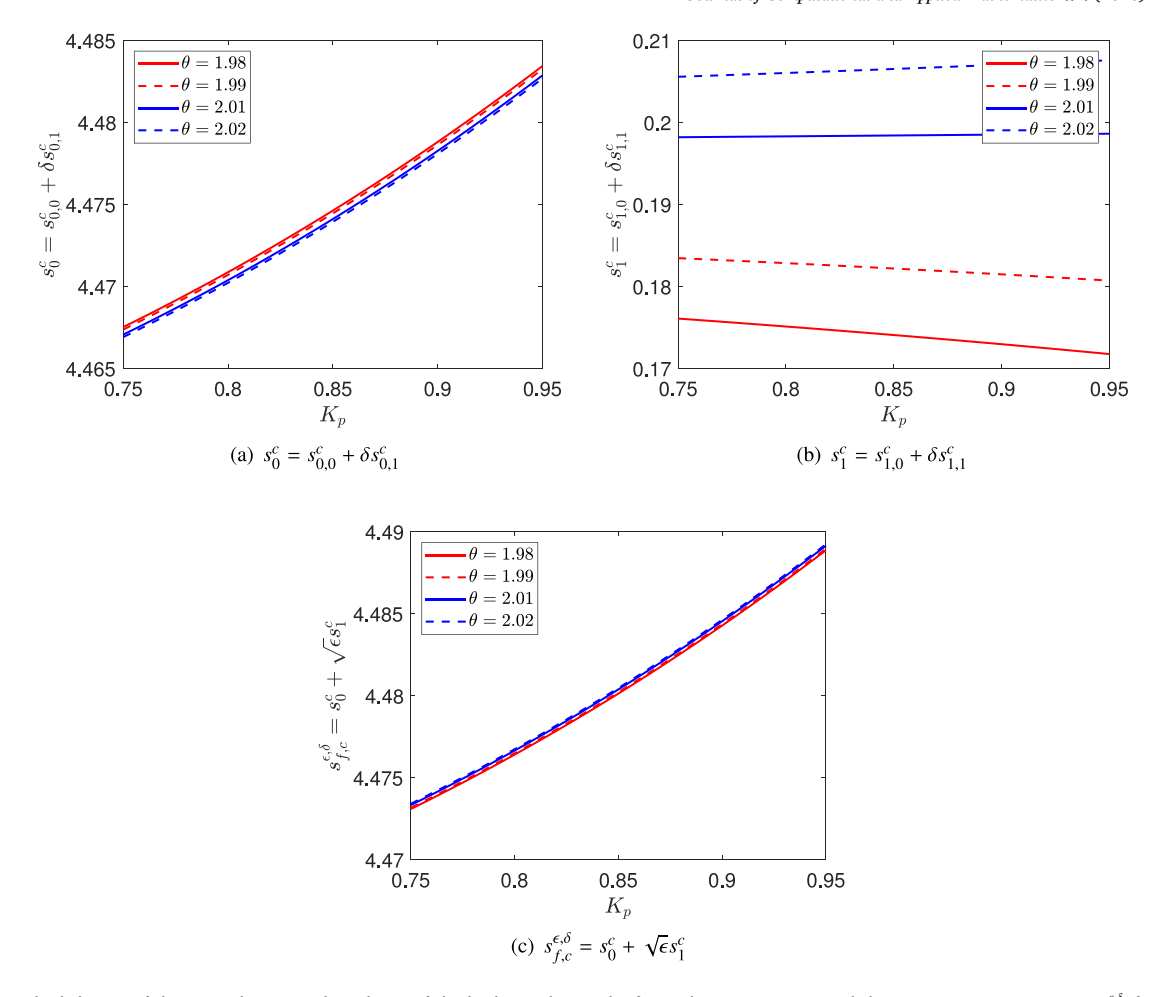


Fig. 2. The behavior of the optimal stopping boundaries of the leading-order  $s_0^c$ , the first-order correction  $s_1^c$ , and the asymptotic approximation  $s_{f,c}^{c,\delta}$  for a call option under the PASO-SVCEV model, examined with respect to the parameter  $K_\rho$ . The red solid line, red dashed line, blue solid line, and blue dashed line correspond to elasticity values  $\theta = 1.98$ , 1.99, 2.01, and 2.02, respectively.

Notes: The underlying asset price is set to the midpoint between  $p_{0,0}$  and  $c_{0,0}$ , and all other parameters are identical to those used in Fig. 1, except for the variation in  $\theta$  and  $K_p$ .

**Theorem 3.6.** For all  $k \ge 1$ , the correction term  $Q_{1,k}$  satisfies the following hierarchy of ODE:

$$\begin{split} &\mathcal{L}_{\text{BS}}Q_{1,k} = G_{1,k} \quad for \ x \in (p_{0,0},c_{0,0}), \\ &\frac{\mathrm{d}Q_{1,k-1}}{\mathrm{d}x}(c_{0,0})c_{1,k} + Q_{1,k}(c_{0,0}) = c_{1,k}e^{c_{0,0}} \\ &\frac{\mathrm{d}Q_{1,k-1}}{\mathrm{d}x}(p_{0,0})p_{1,k} + Q_{1,k}(p_{0,0}) = -p_{1,k}e^{p_{0,0}} \\ &\frac{\mathrm{d}^2Q_{1,k-1}}{\mathrm{d}x^2}(c_{0,0})c_{1,k} + \frac{\mathrm{d}Q_{1,k}}{\mathrm{d}x}(c_{0,0}) = c_{1,k}e^{c_{0,0}} \\ &\frac{\mathrm{d}^2Q_{1,k-1}}{\mathrm{d}x^2}(p_{0,0})p_{1,k} + \frac{\mathrm{d}Q_{1,k}}{\mathrm{d}x}(p_{0,0}) = -p_{1,k}e^{p_{0,0}}, \end{split} \tag{3.36}$$

where the non-homogeneous term  $G_{1k}$  is given by

$$\begin{split} G_{1,k} = & \frac{1}{2} \bar{\sigma}^2 \sum_{i=1}^k \frac{(-1)^{i+1} x^i}{i!} \left( \frac{\mathrm{d}^2 Q_{1,k-i}}{\mathrm{d} x^2} - \frac{\mathrm{d} Q_{1,k-i}}{\mathrm{d} x} \right) + \frac{\sqrt{2}}{2} \rho u \langle f(y) \phi'(y) \rangle \frac{(-3)^k x^k}{2^k k!} \frac{\mathrm{d}^3 Q_{0,0}}{\mathrm{d} x^3} \\ & + \frac{1}{\sqrt{2}} u \left( \rho \langle f \phi' \rangle \frac{(-3)^{k+1} x^k}{2^k k!} + \rho \langle f \phi' \rangle \frac{3^k x^k}{2^{k-1} k!} - \rho \langle f \phi' \rangle \frac{3^{k-1} x^{k-1}}{2^{k-1} (k-1)!} - \langle \Lambda \phi' \rangle \frac{(-1)^k x^k}{k!} \right) \frac{\mathrm{d}^2 Q_{0,0}}{\mathrm{d} x^2} \\ & - \frac{1}{\sqrt{2}} u \left( -\rho \langle f \phi' \rangle \frac{(-3)^k x^k}{2^k k!} + \rho \langle f \phi' \rangle \frac{3^k x^k}{2^{k-1} k!} - \rho \langle f \phi' \rangle \frac{3^{k-1} x^{k-1}}{2^{k-1} (k-1)!} - \langle \Lambda \phi' \rangle \frac{(-1)^k x^k}{k!} \right) \frac{\mathrm{d} Q_{0,0}}{\mathrm{d} x}. \end{split}$$

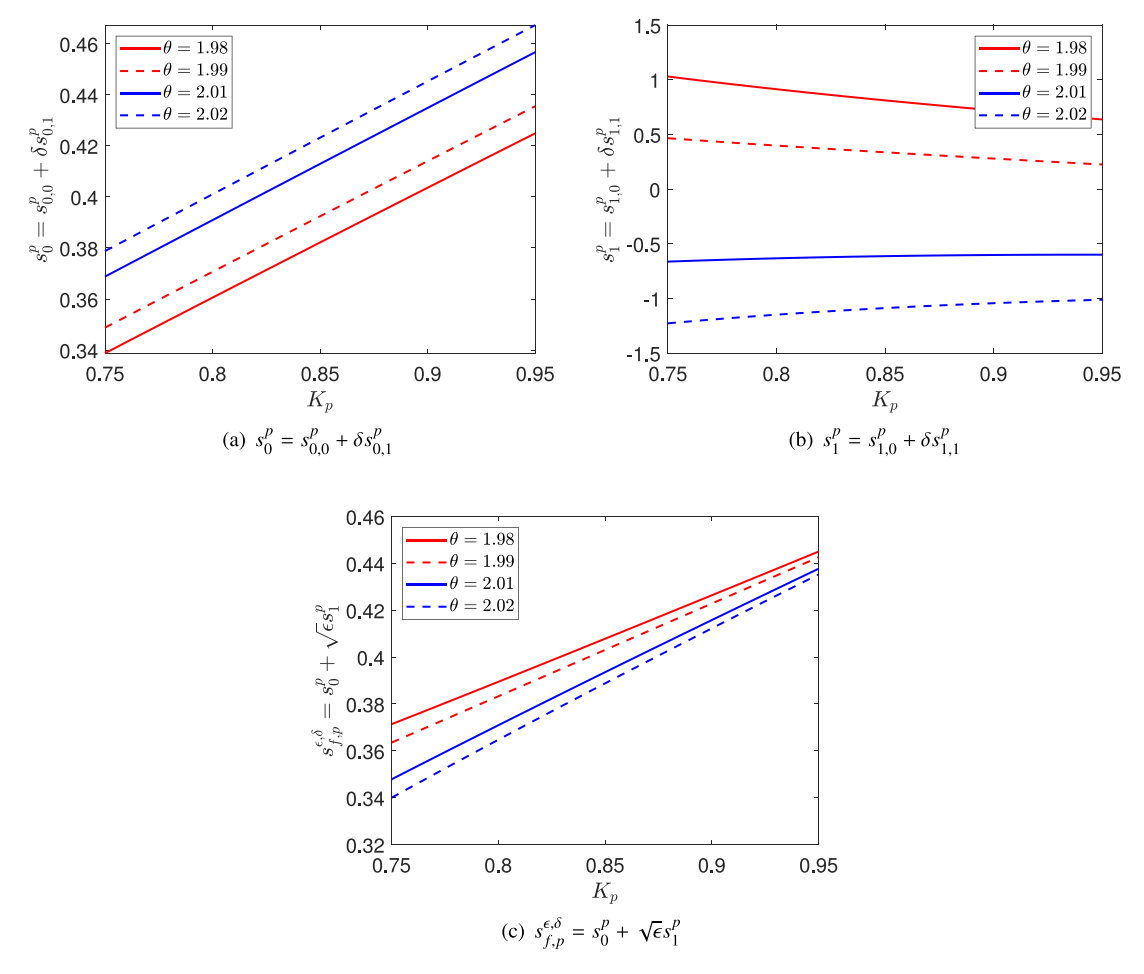


Fig. 3. The behavior of the optimal stopping boundaries of the leading-order  $s_0^p$ , the first-order correction  $s_1^p$ , and the asymptotic approximation  $s_{f,p}^{\varepsilon,\delta}$  for a put option under the PASO-SVCEV model, examined with respect to the parameter  $K_p$ . The red solid line, red dashed line, blue solid line, and blue dashed line correspond to elasticity values  $\theta = 1.98$ , 1.99, 2.01, and 2.02, respectively.

Notes: All parameters are identical to those used in Fig. 2.

Then, the solution  $Q_{1,k}$  of PDE (3.36) is given by

$$Q_{1,k} = C_9 e^{\lambda_1 x} + C_{10} e^{\lambda_2 x} - e^{\lambda_1 x} \int_{p_{0.0}}^{x} \frac{e^{\lambda_2 z} G_{1,k}}{(\lambda_2 - \lambda_1) e^{(\lambda_1 + \lambda_2) z}} dz + e^{\lambda_2 z} \int_{p_{0.0}}^{x} \frac{e^{\lambda_1 z} G_{1,k}}{(\lambda_2 - \lambda_1) e^{(\lambda_1 + \lambda_2) z}} dz, \tag{3.37}$$

where  $\lambda_1 > 0$  and  $\lambda_2 < 0$  are two real roots of the quadratic equation (3.19). Furthermore, the correction terms for the free boundaries  $c_{1,k}$  and  $p_{1,k}$  are determined by

$$\begin{split} c_{1,k} &= \frac{1}{d} \left[ B_{11} \left( e^{\lambda_1 c_{0,0}} D_9 + e^{\lambda_2 c_{0,0}} D_{10} \right) + B_{12} \left( e^{\lambda_1 p_{0,0}} D_9 + e^{\lambda_2 p_{0,0}} D_{10} \right) \right. \\ &\quad \left. + B_{13} \left( -e^{\lambda_1 c_{0,0}} \left( \lambda_1 D_9 + \widehat{D}_7 \right) + e^{\lambda_2 c_{0,0}} \left( \lambda_2 D_{10} + \widehat{D}_8 \right) \right) + B_{14} \left( e^{\lambda_1 p_{0,0}} \left( -\lambda_1 D_9 + \widetilde{D}_7 \right) + e^{\lambda_2 p_{0,0}} \left( \lambda_2 D_{10} + \widetilde{D}_8 \right) \right) \right], \\ p_{1,k} &= \frac{1}{d} \left[ B_{21} \left( e^{\lambda_1 c_{0,0}} D_9 + e^{\lambda_2 c_{0,0}} D_{10} \right) + B_{22} \left( e^{\lambda_1 p_{0,0}} D_9 + e^{\lambda_2 p_{0,0}} D_{10} \right) \right. \\ &\quad \left. + B_{23} \left( -e^{\lambda_1 c_{0,0}} \left( \lambda_1 D_9 + \widehat{D}_7 \right) + e^{\lambda_2 c_{0,0}} \left( \lambda_2 D_{10} + \widehat{D}_8 \right) \right) + B_{24} \left( e^{\lambda_1 p_{0,0}} \left( -\lambda_1 D_9 + \widetilde{D}_7 \right) + e^{\lambda_2 p_{0,0}} \left( \lambda_2 D_{10} + \widetilde{D}_8 \right) \right) \right], \end{split}$$

where

$$\begin{split} D_9 &= \int_{\rho_{0,0}}^{c_{0,0}} \frac{e^{\lambda_2 z} G_{1,k}}{(\lambda_2 - \lambda_1) e^{(\lambda_1 + \lambda_2) z}} \mathrm{d}z, \qquad \widehat{D}_9 = \frac{e^{\lambda_2 c_{0,0}} G_{1,k}}{(\lambda_2 - \lambda_1) e^{(\lambda_1 + \lambda_2) c_{0,0}}}, \qquad \widetilde{D}_9 = \frac{e^{\lambda_2 \rho_{0,0}} G_{1,k}}{(\lambda_2 - \lambda_1) e^{(\lambda_1 + \lambda_2) \rho_{0,0}}}, \\ D_{10} &= \int_{\rho_{0,0}}^{c_{0,0}} \frac{e^{\lambda_1 z} G_{1,k}}{(\lambda_2 - \lambda_1) e^{(\lambda_1 + \lambda_2) z}} \mathrm{d}z, \qquad \widehat{D}_{10} = \frac{e^{\lambda_2 c_{0,0}} G_{1,k}}{(\lambda_2 - \lambda_1) e^{(\lambda_1 + \lambda_2) c_{0,0}}}, \qquad \widetilde{D}_{10} = \frac{e^{\lambda_2 \rho_{0,0}} G_{1,k}}{(\lambda_2 - \lambda_1) e^{(\lambda_1 + \lambda_2) \rho_{0,0}}}, \end{split}$$

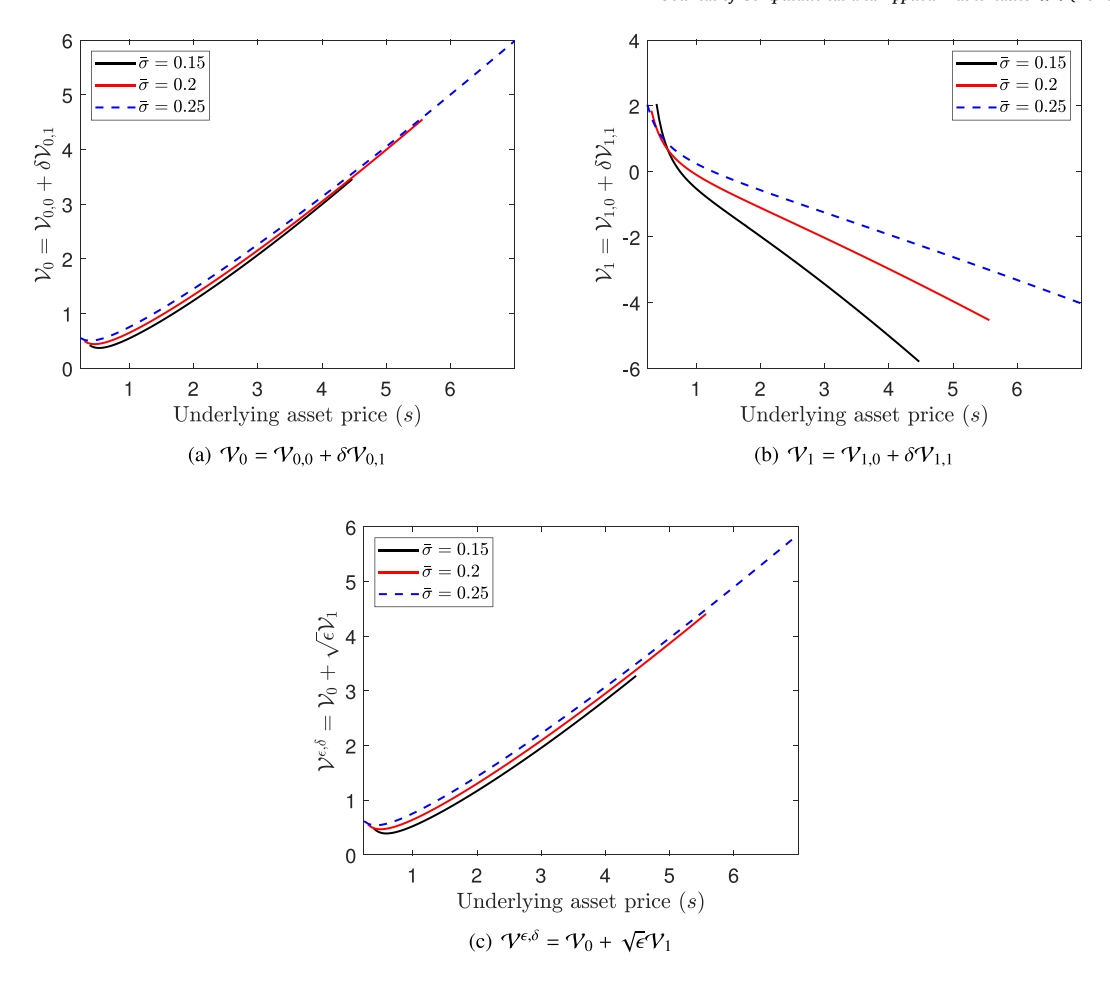


Fig. 4. The dynamics of the leading-order term  $V_0$ , the correction term  $V_1$ , and the asymptotic approximation  $V^{e,\delta}$  under the PASO-SVCEV model, plotted as functions of the risky asset price for a given effective volatility. The black solid line, red line, and blue dashed line correspond to effective volatility values  $\bar{\sigma} = 0.15$ , 0.2, and 0.25, respectively.

Notes: The elasticity parameter is fixed at  $\theta=1.99$ , and all other parameters are identical to those used in Fig. 1, except for variations in  $\bar{\sigma}$  and  $K_{\rho}$ .

$$\begin{split} C_9 &= \frac{1}{d} \left[ B_{31} \left( e^{\lambda_1 c_{0,0}} D_9 + e^{\lambda_2 c_{0,0}} D_{10} \right) + B_{32} \left( e^{\lambda_1 p_{0,0}} D_9 + e^{\lambda_2 p_{0,0}} D_{10} \right) \right. \\ &\quad \left. + B_{33} \left( - e^{\lambda_1 c_{0,0}} \left( \lambda_1 D_9 + \widehat{D}_9 \right) + e^{\lambda_2 c_{0,0}} \left( \lambda_2 D_{10} + \widehat{D}_{10} \right) \right) + B_{34} \left( e^{\lambda_1 p_{0,0}} \left( -\lambda_1 D_9 + \widetilde{D}_9 \right) + e^{\lambda_2 p_{0,0}} \left( \lambda_2 D_{10} + \widetilde{D}_{10} \right) \right) \right], \\ C_{10} &= \frac{1}{d} \left[ B_{41} \left( e^{\lambda_1 c_{0,0}} D_9 + e^{\lambda_2 c_{0,0}} D_{10} \right) + B_{42} \left( e^{\lambda_1 p_{0,0}} D_9 + e^{\lambda_2 p_{0,0}} D_{10} \right) \right. \\ &\quad \left. + B_{43} \left( - e^{\lambda_1 c_{0,0}} \left( \lambda_1 D_9 + \widehat{D}_7 \right) + e^{\lambda_2 c_{0,0}} \left( \lambda_2 D_{10} + \widehat{D}_{10} \right) \right) + B_{44} \left( e^{\lambda_1 p_{0,0}} \left( -\lambda_1 D_9 + \widetilde{D}_9 \right) + e^{\lambda_2 p_{0,0}} \left( \lambda_2 D_{10} + \widetilde{D}_{10} \right) \right) \right]. \end{split}$$

Also, d and  $B_{i,j}$  for  $1 \le i, j \le 4$  are defined in Theorem 3.2.

**Proof.** The proof is similar to that of Theorem 3.2. As mentioned in the previous theorem, the ODE given in Eq. (3.36) is reformulated as a Cauchy–Euler equation, resulting in the formula  $Q_{1k}$  given in (3.37).

Herein, from Theorems 3.1, 3.2, 3.4, and 3.5, the option price V given by combining (3.18), (3.22), (3.32), and (3.35) can be approximated by

$$\mathcal{V} \approx \mathcal{V}^{\epsilon,\delta} := \mathcal{V}_0 + \sqrt{\epsilon} \mathcal{V}_1 := \mathcal{V}_{0,0} + \delta \mathcal{V}_{0,1} + \sqrt{\epsilon} \left( \mathcal{V}_{1,0} + \delta \mathcal{V}_{1,1} \right). \tag{3.38}$$

Similarly, the free boundaries  $s_{f,c}$  and  $s_{f,p}$  given in Theorems 3.1, 3.2, 3.4, and 3.5 can be approximated by

$$s_{f,c} \approx s_{f,c}^{\epsilon,\delta} := s_0^c + \sqrt{\epsilon} s_1^c := s_{0,0}^c + \delta s_{0,1}^c + \sqrt{\epsilon} \left( s_{1,0}^c + \delta s_{1,1}^c \right), \tag{3.39}$$

$$s_{f,p} \approx s_{f,p}^{\epsilon,\delta} := s_0^p + \sqrt{\epsilon} s_1^p := s_{0,0}^p + \delta s_{0,1}^p + \sqrt{\epsilon} \left( s_{1,0}^p + \delta s_{1,1}^p \right), \tag{3.40}$$

respectively. The accuracy of these approximations is theoretically verified in the following theorem.

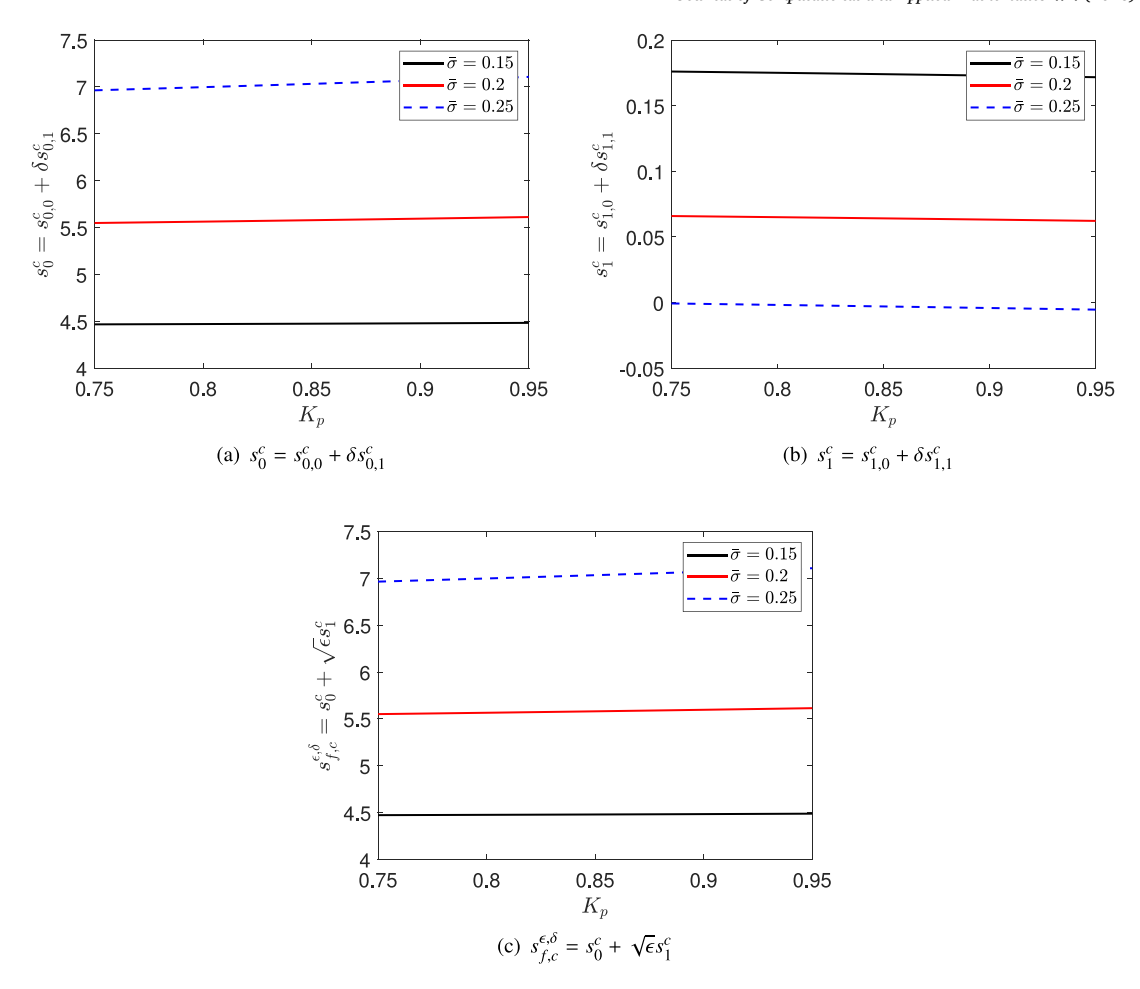


Fig. 5. The behavior of the optimal stopping boundaries of the leading-order  $s_0^c$ , the first-order correction  $s_1^c$ , and the asymptotic approximation  $s_{f,c}^{c,\delta}$  for a call option under the PASO-SVCEV model, examined with respect to the parameter  $K_p$  for a given effective volatility. The black solid line, red line, and blue dashed line correspond to effective volatility values  $\bar{\sigma} = 0.15$ , 0.2, and 0.25, respectively.

Notes:  $s = (p_{0.0} + c_{0.0})/2$ ,  $\theta = 1.99$ ; all other parameters match those in Fig. 1, except for changes in  $\bar{\sigma}$  and  $K_p$ .

**Theorem 3.7** (Accuracy of Option Price and Free Boundaries). Consider  $V^{\epsilon,\delta}$  as the first-order approximation price of PASO under the SVCEV framework given by (3.38). Assuming that the payoff function h is smooth everywhere except at the strike prices  $K_p$  and  $K_c$ , the accuracy of the price of PASO-SVCEV is expressed as:

$$\left| \mathcal{V} - \mathcal{V}^{\epsilon, \delta} \right| = \mathcal{O}(\epsilon, \delta).$$
 (3.41)

Similarly, let  $s_{f,c}(v)$  and  $s_{f,p}(v)$  denote the respective free boundaries for the call and put options in PASO-SVCEV, as given in PDE (2.5). First-order approximations for the free boundaries are defined by (3.39) and (3.40). Assuming that the payoff function h is continuously differentiable and bound; in that case, the accuracy for the free boundaries  $s_{f,c}$  and  $s_{f,p}$  is described by

$$\left|s_{f,c}(v) - s_{f,c}^{\epsilon,\delta}\right| = \mathcal{O}(\epsilon,\delta), \quad \text{and} \quad \left|s_{f,p}(v) - s_{f,p}^{\epsilon,\delta}\right| = \mathcal{O}(\epsilon,\delta). \tag{3.42}$$

**Proof.** The PDE (2.5) can be converted into PDE (2.10) using the same change of variable method introduced in Section 2. We can derive the first-order term approximation  $Q(x,v) \approx Q_{0,0}(x) + \delta Q_{0,1}(x) + \sqrt{\epsilon} \left(Q_{1,0}(x) + \delta Q_{1,1}(x)\right)$  by applying the asymptotic method presented in Section 3, where  $Q_{0,0}$  represents the leading order price, as defined in (3.18), and  $Q_{0,1}$ ,  $Q_{1,1}$ , and  $Q_{1,1}$  are the correction terms provided in Theorems 3.2, 3.4, and 3.5, respectively. Similarly, the first-order approximations of the optimal boundaries  $x_{f,c}$  and  $x_{f,p}$  are given by  $x_{f,p}(v) \approx p_{0,0} + \delta p_{0,1} + \sqrt{\epsilon}(p_{1,0} + \delta p_{1,1})$  and  $x_{f,c}(v) \approx c_{0,0} + \delta c_{0,1} + \sqrt{\epsilon}(c_{1,0} + \delta c_{1,1})$ . Each term in these expressions corresponds to specific components derived from theoretical analysis. Then, using the change of variable,  $x = \ln s$ ,  $x_{f,c} = \ln s_{f,c}$  and  $x_{f,p} = \ln s_{f,p}$ , these results can be reformulated as the approximation price in (3.38), and the approximation of free boundaries in (3.39) and (3.40). Detailed proofs are provided in [8,33].

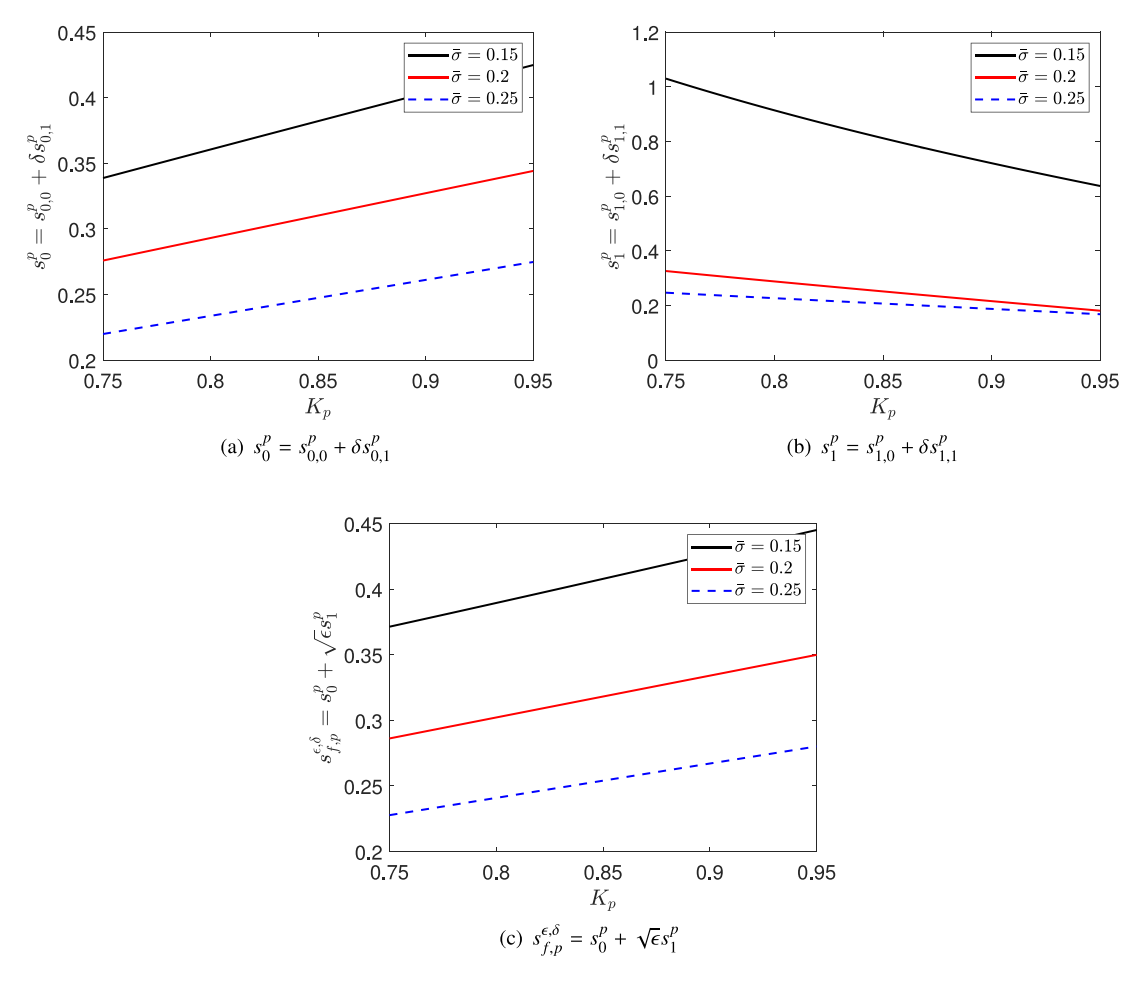


Fig. 6. The behavior of the optimal stopping boundaries of the leading-order  $s_p^0$ , the first-order correction  $s_1^p$ , and the asymptotic approximation  $s_{f,p}^{c,\delta}$  for a put option under the PASO-SVCEV model, examined with respect to the parameter  $K_p$  for a given effective volatility. The black solid line, red line, and blue dashed line correspond to effective volatility values  $\bar{\sigma} = 0.15$ , 0.2, and 0.25, respectively.

Notes: All parameters are identical to those used in Fig. 5.

#### 4. Numerical implications

In this section, we investigate the price changes of perpetual American strangle options under the SVCEV model (PASO-SVCEV) with regard to the model parameters. For the numerical analysis, in (3.38)–(3.40), we mentioned the approximated option prices

$$\mathcal{V}^{\epsilon,\delta} := \mathcal{V}_0 + \sqrt{\epsilon}\mathcal{V}_1 := \mathcal{V}_{0,0} + \delta\mathcal{V}_{0,1} + \sqrt{\epsilon}(\mathcal{V}_{1,0} + \delta\mathcal{V}_{1,1}), \tag{4.1}$$

and

$$s_{f,c}^{\epsilon,\delta} := s_0^c + \sqrt{\epsilon} s_1^c := s_{0,0}^c + \delta s_{0,1}^c + \sqrt{\epsilon} \left( s_{1,0}^c + \delta s_{1,1}^c \right), \tag{4.2}$$

$$s_{f,p}^{\epsilon,\delta} := s_0^p + \sqrt{\epsilon} s_1^p := s_{0,0}^p + \delta s_{0,1}^p + \sqrt{\epsilon} \left( s_{1,0}^p + \delta s_{1,1}^p \right). \tag{4.3}$$

In Table 1, as described by Choi et al. [10], the historical data analysis of the volatility of the S&P 500 index reveals that the elasticities are close to 2. Thus, the corrected price of the PASO under the SVCEV model given by (4.1) is reasonable for the numerical experiments in this section.

In the numerical analysis, we investigate the pricing accuracy of the approximation formula for PASO-SVCEV using the Monte Carlo method. Monte Carlo simulations were conducted using 10,000 simulated paths for the underlying asset price. In addition, according to Ha et al. [27], we select the baseline parameters as follows: s = 0.9, v = 0,  $K_p = 0.8$ ,  $K_c = 1.0$ , r = 0.03, q = 0.01, m = -1.8594, u = 0.5,  $\rho = -0.2$ ,  $\bar{\sigma} = 0.15$ ,  $\langle f(v)\phi'(v)\rangle = 0.1$ , and  $\langle \Lambda(v)\phi'(v)\rangle = 0.8266$ .

Table 1 presents the results of the Monte-Carlo simulation, comparing Monte Carlo simulated option prices  $\mathcal{V}_{MC}$  and the corrected approximation formula  $\mathcal{V}^{\epsilon,\delta}$  with respect to  $\epsilon$  and  $\theta$ . Table 1 also highlights the absolute errors  $|\mathcal{V}_{MC} - \mathcal{V}_{0,0}|$ ,  $|\mathcal{V}_{MC} - \mathcal{V}^{\epsilon,\delta}|$ , and the relative errors RE<sub>1</sub> and RE<sub>2</sub> for each parameter sets. In addition, time<sub>1</sub> represents the computation time required for the Monte Carlo

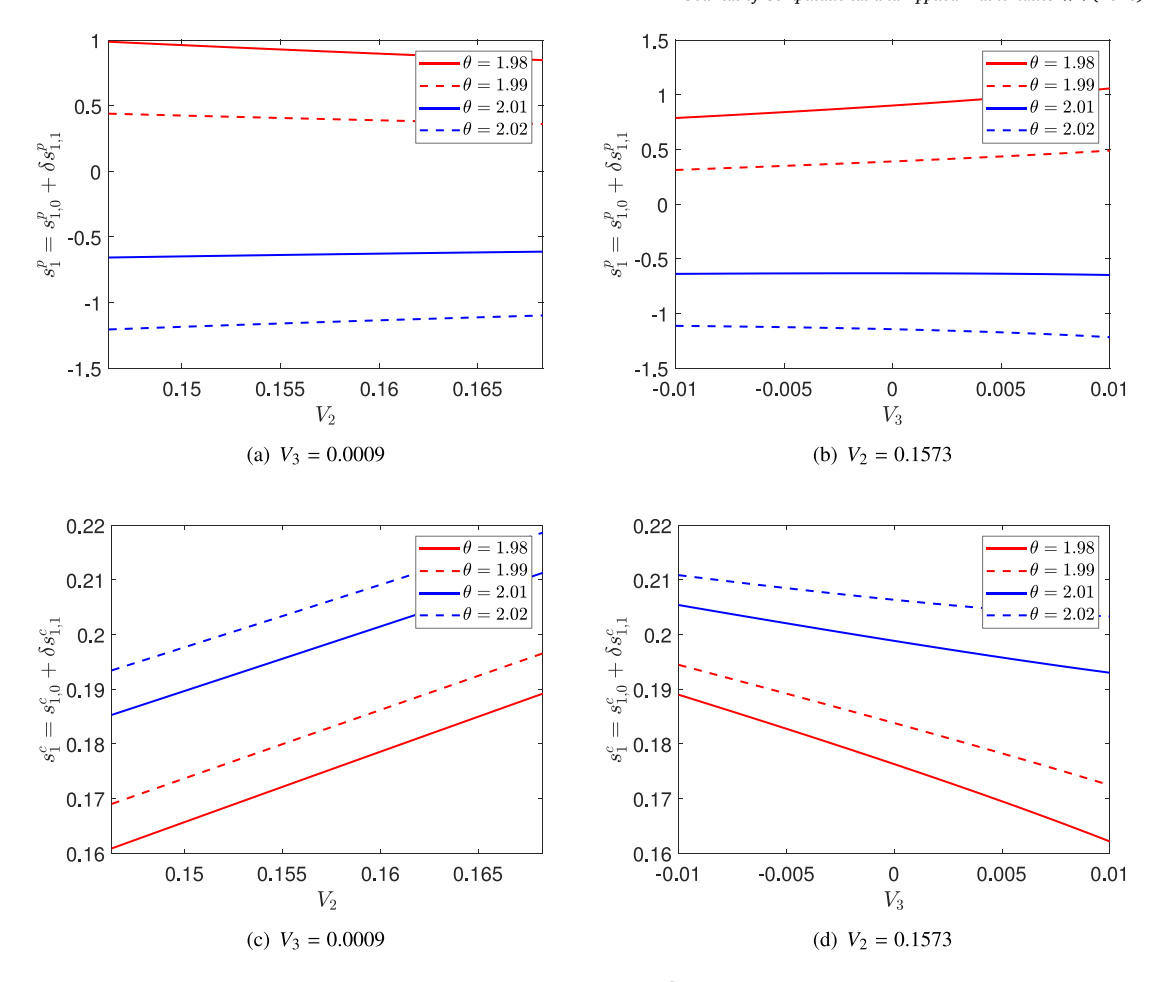


Fig. 7. The dynamics of the optimal stopping boundaries of the correction terms  $s_1^c$  and  $s_1^p$  under the PASO-SVCEV model, shown as functions of the grouped parameters  $V_2$  and  $V_3$ , respectively, for given elasticity values. The red solid line, red dashed line, blue solid line, and blue dashed line correspond to elasticity values  $\theta = 1.98, 1.99, 2.01$ , and 2.02, respectively.

Notes: All parameters are identical to those used in Fig. 1, except for the variation in  $V_2$ ,  $V_3$ , and  $\theta$ .

simulation, while time<sub>2</sub> denotes the time taken by the proposed approximation method. We examine and compare the computational costs of both approaches, and found that the first-order approximated price can be obtained significantly faster than the Monte Carlo-based result. As the parameter  $\epsilon$  decreases, the price difference between the corrected approximation formula  $\mathcal{V}^{\epsilon,\delta}$  and the Monte-Carlo price  $\mathcal{V}_{MC}$  approaches zero, with the relative error consistently decreasing for each elasticity value  $\theta$ . Consequently, with the increasing number of simulations, the numerical solution provided by the Monte-Carlo simulation, which is considered the best approximation of a real-world solution, approaches the approximated price given by (4.1). This result suggests that the analytic option price presented in Theorem 3.7 or (4.1) becomes an accurate solution for PASO-SVCEV.

Fig. 1 illustrates the pricing behaviors of the leading-order term  $V_0$ , the correction term  $V_1$ , and the approximated solution  $V_0 + \sqrt{\epsilon}V_1$  for PASO-SVCEV with respect to the underlying asset value for an elasticity parameter  $\theta$ . Fig. 1(a) reveals that  $V_0$  exhibits an increasing trend in option prices as the underlying asset price rises, regardless of the value of  $\theta$ . In Fig. 1(b),  $V_1$  displays diffusing patterns when the risky asset is near the strike price of the call or put option against the value of  $\theta$ . Particularly, for the elasticity parameter, the price impact of  $V_0$  remains almost unchanged; however, that of  $V_1$  tends to be sensitive to the risky asset value near the strike prices  $K_\rho$  and  $K_c$ . This observation indicates that the price sensitivity for the correction term embedded in the SV exceeds that of the leading-order term for the elasticity  $\theta$  as the underlying asset approaches the strike prices of the call or put option. This implies that the effect of SV on the option price is substantial in terms of the elasticity value of the underlying asset near the strike prices of the call or put option. Thus, in Fig. 1(c), the price difference between the approximated option values for the elasticity parameter becomes larger than that of the leading-order values.

Figs. 2 and 3 present the pricing behaviors of the leading order term  $(s_0^c \text{ or } s_0^p)$ , the correction term  $(s_1^c \text{ or } s_1^p)$ , and the approximated value  $(s_{f,c}^{\epsilon,\delta} \text{ or } s_{f,p}^{\epsilon,\delta})$  for the optimal stopping boundaries of the call or put option on PASO-SVCEV with regards to  $K_p$  for a given elasticity value. In both figures, the price effect of the correction terms increases more than that of the leading order terms against the given elasticity parameter. This implies that the free-boundary values for the call or put option for PASO-SVCEV

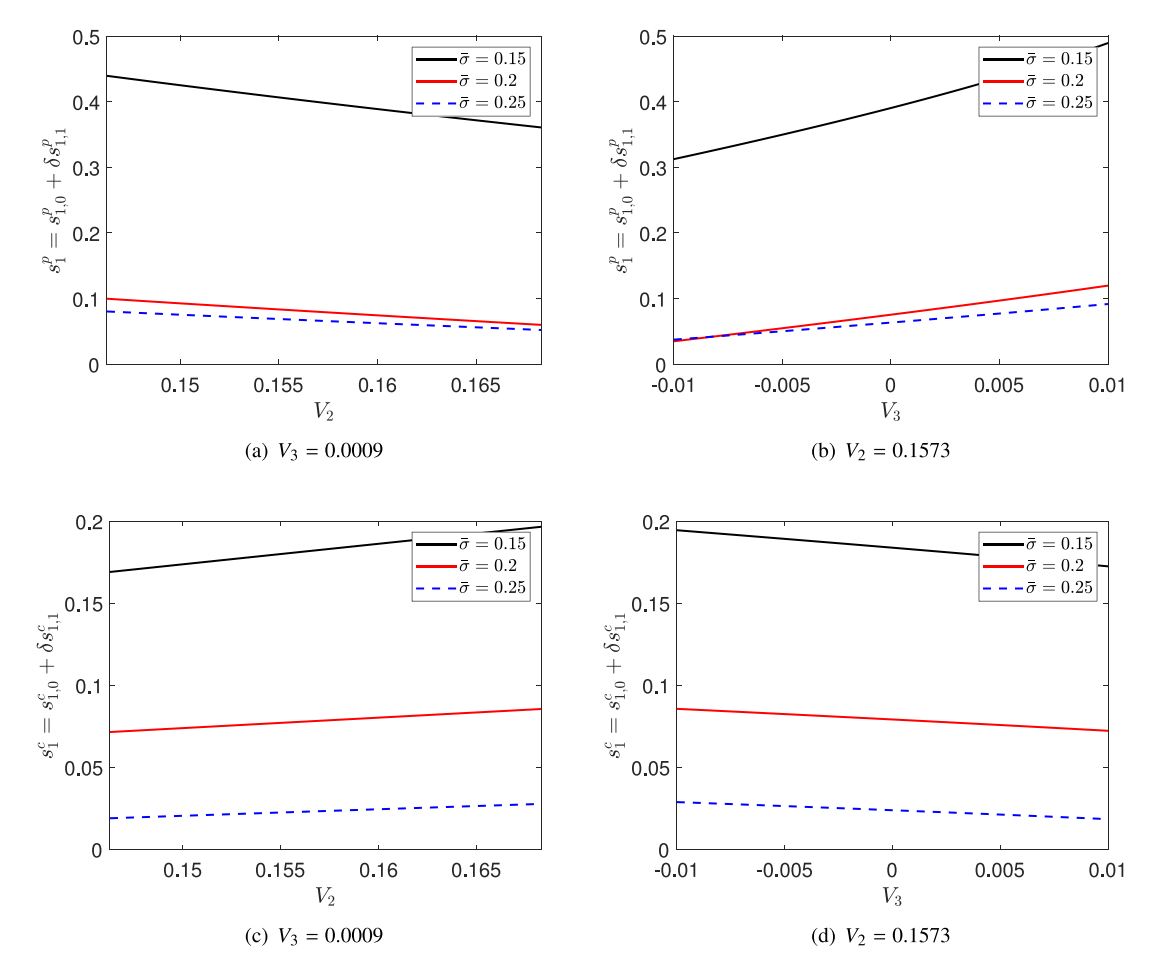


**Fig. 8.** The dynamics of the optimal stopping boundaries of the correction terms  $s_1^c$  and  $s_1^p$  under the PASO-SVCEV model, shown as functions of the grouped parameters  $V_2$  and  $V_3$ , respectively, for given effective volatility. The black solid line, red line, and blue dashed line correspond to effective volatility values  $\bar{\sigma} = 0.15$ , 0.2, and 0.25, respectively.

Notes:  $s = (p_{0,0} + c_{0,0})/2$ ,  $\theta = 1.99$ ; all other parameters match those in Fig. 1, except for changes in  $V_2$ ,  $V_3$ , and  $\bar{\sigma}$ .

are significantly influenced by the SV factor for the elasticity value. The pricing impact of the correction-order term  $s_1^p$  is more substantial than that of the correction-order value  $s_1^c$  for the elasticity parameter. Consequently, the effect of SV on the option price is substantial in the optimal boundaries of the put option rather than those of the call option. This indicates that for both approximated prices of the optimal boundary, the price gap of the corrected value for the put option is larger than that for the call option.

Fig. 4 illustrates the pricing changes of the leading-order term  $\mathcal{V}_0$ , the correction term  $\mathcal{V}_1$ , and the approximated value  $\mathcal{V}^{\epsilon,\delta}$  for PASO-SVCEV in terms of the risky asset price for a given effective volatility. The Figures reveal that the correction-order term price  $\mathcal{V}_1$  is more sensitive than the leading-order term price  $\mathcal{V}_0$  with respect to the effective volatility. This suggests that the impact of the correction term, which is closely related to the SV on the option price, is highly sensitive to the influence of the leading-order term with respect to the volatility value. In addition, the price influence of the correction term becomes substantial with decreasing volatility. Furthermore, the payoff of a strangle option can generate substantial returns from the investment, regardless of whether the underlying asset price rises or falls drastically because it combines the characteristics of call and put options. Thus, suppose that the volatility is low; in that case, the potential profits from the investment decrease, ultimately resulting in a relatively higher investment risk. Consequently, as volatility decreases, the price influence on the option becomes more sensitive to the underlying asset.

Figs. 5 and 6 display the pricing sensitivities of the leading order term  $(s_0^c \text{ or } s_0^p)$ , the correction term  $(s_1^c \text{ or } s_1^p)$  and the approximated price  $(s_{f,c}^{\epsilon,\delta} \text{ or } s_{f,p}^{\epsilon,\delta})$  for the free boundaries of the call or put options on PASO-SVCEV in terms of  $K_p$  for a given effective volatility. Comparing the optimal stopping boundaries of the call and put options, the volatility of the free boundaries of the call option exhibits minimal changes in the prices for  $s_0^c$ ,  $s_1^c$ , and  $s_{f,c}^{\epsilon,\delta}$ . However, the price changes for  $s_0^p$ ,  $s_1^p$ , and  $s_{f,p}^{\epsilon,\delta}$  are substantial and more prominent than those of the free-boundaries of the call option. Furthermore, as opposed to the optimal stopping boundaries of the call option, the price impact of the correction term increases more than that of the leading order term in the free boundary of

Table 1
The error comparison between the Monte-Carlo price for (denoted by  $\mathcal{V}_{\text{MC}}$ ) and the corrected formula ( $\mathcal{V}^{\epsilon,\delta}$ ) with respect to  $\epsilon$  and simulation number 10,000. Notes: The parameters used for this table are:  $s=0.9, v=0, r=0.03, q=0.01, \bar{\sigma}=0.15, K_{\epsilon}=1.0, K_{p}=0.8, u=0.5, m=-1.8594, \rho_{xv}=-0.2, \langle f(v)\phi'(v)\rangle=0.1, \langle A(v)\phi'(v)\rangle=0.8266.$ 

θ	$\epsilon$	$\mathcal{V}_{\mathrm{MC}}$	CI	$\mathcal{V}_{0,0}$	$\mathcal{V}^{\epsilon,\delta}$	$\left \mathcal{V}_{MC}-\mathcal{V}_{0,0}\right $	$ \mathcal{V}_{\mathrm{MC}} - \mathcal{V}^{\epsilon,\delta} $	RE <sub>1</sub> [%]	RE <sub>2</sub> [%]	time <sub>1</sub> [s]	time <sub>2</sub> [s]
2.02	0.0100	0.429093	[0.425957, 0.432229]	0.485250	0.393425	0.056157	0.035668	13.087482	8.312429	0.031478	122.069102
	0.0050	0.442743	[0.439106, 0.446381]	0.485250	0.418232	0.042507	0.024512	9.600775	5.536291	0.031478	120.966143
	0.0010	0.456751	[0.452484, 0.461017]	0.485250	0.451338	0.028499	0.005413	6.239575	1.185078	0.031478	120.307276
	0.0005	0.463099	[0.458500, 0.467697]	0.485250	0.459183	0.022152	0.003916	4.783364	0.845562	0.031478	107.702800
	0.0001	0.471550	[0.466525, 0.476576]	0.485250	0.469652	0.013700	0.001899	2.905278	0.402614	0.031478	101.953143
2.01	0.0100	0.439964	[0.436744, 0.443184]	0.485250	0.409496	0.045286	0.030468	10.293180	6.925126	0.032315	107.077780
	0.0050	0.456705	[0.452939, 0.460471]	0.485250	0.430640	0.028545	0.026065	6.250218	5.707252	0.032315	113.686849
	0.0010	0.466031	[0.461602, 0.470459]	0.485250	0.458857	0.019220	0.007173	4.124141	1.539186	0.032315	119.882369
	0.0005	0.469497	[0.464893, 0.474101]	0.485250	0.465544	0.015753	0.003953	3.355369	0.842001	0.032315	108.879134
	0.0001	0.477757	[0.472652, 0.482862]	0.485250	0.474467	0.007493	0.003290	1.568453	0.688625	0.032315	101.816397
1.99	0.0100	0.457836	[0.451519, 0.461153]	0.485250	0.441638	0.027414	0.016198	5.987804	3.537897	0.031322	119.504278
	0.0050	0.462787	[0.459030, 0.466544]	0.485250	0.455456	0.022463	0.007331	4.853838	1.584201	0.031322	111.977774
	0.0010	0.477945	[0.473505, 0.482386]	0.485250	0.473896	0.007305	0.004049	1.528441	0.847176	0.031322	115.045335
	0.0005	0.480434	[0.475705, 0.485162]	0.485250	0.478266	0.004817	0.002168	1.002565	0.451251	0.031322	102.098709
	0.0001	0.484617	[0.479522, 0.489711]	0.485250	0.484097	0.000634	0.000520	0.130762	0.107219	0.031322	101.089543
1.98	0.0100	0.465610	[0.462543, 0.469686]	0.485250	0.457709	0.019640	0.007901	4.218092	1.696929	0.030702	106.738700
	0.0050	0.474827	[0.471194, 0.478460]	0.485250	0.467864	0.010423	0.006963	2.195130	1.466507	0.030702	111.583636
	0.0010	0.476667	[0.472232, 0.481103]	0.485250	0.481415	0.008583	0.004748	1.800625	0.996121	0.030702	122.092209
	0.0005	0.481150	[0.476459, 0.485841]	0.485250	0.484627	0.004100	0.003477	0.852163	0.722542	0.030702	113.935380
	0.0001	0.488279	[0.486995, 0.496261]	0.485250	0.488912	0.003029	0.000633	0.620293	0.129634	0.030702	113.516048

the put option for effective volatility. This implies that the free boundaries on the option value are more influenced by the volatility in the optimal boundaries for the put options than for call options. This highlights that the effect of SV on the free boundary is highly sensitive to the volatility in the optimal boundaries of the put option rather than those of the call option.

Fig. 7 exhibits the pricing changes of the correction terms  $s_1^\rho$  and  $s_1^\rho$  for PASO-SVCEV with respect to the group parameters  $V_2$  or  $V_3$  for the elasticity parameter, where the group parameters are defined as  $V_2 := \sqrt{2}\rho u \langle f(y)\phi'(y)\rangle - \frac{\sqrt{2}}{2}u \langle \Lambda(y)\phi'(y)\rangle$  and  $V_3 := \frac{\sqrt{2}}{2}\rho u \langle f(y)\phi'(y)\rangle$ . The group parameter  $V_3$  involves the correlation between the underlying asset and volatility,  $\rho$ , and the group parameter  $V_2$  involves the market price of risk  $V_3$  indicating that  $V_3$  are closely linked to  $V_3$  and  $V_3$  are represented to the put option increases more than that of the call option against the group parameters  $V_3$  or  $V_3$  as the elasticity varies. This implies that the effect of SV on the optimal-boundary price for the put option is greater compared to that of the call option with respect to the group parameter  $V_3$  or  $V_3$ .

Fig. 8 displays the price changes of the correction terms  $s_1^c$  and  $s_1^p$  for PASO-SVCEV in terms of the group parameters  $V_2$  or  $V_3$  for the given effective volatility. Similar to Fig. 7, when the correction term value  $s_1^c$  and the correction term price  $s_1^p$  are compared, the pricing sensitivities of the correction term of the free boundary for the put option exceed those of the correction term for the call option for the given effective volatility. Thus, most investors in the financial market react more sensitively to declines in underlying assets than to increases. In such cases, investors holding strangle options can still expect to benefit considerably from the put option embedded in the payoff, even during a bear market. Therefore, the free-boundary value of the put option with the value of the relatively high expectation in the bear market may have greater impacts than those of the call option of the relatively low expectation. Therefore, the effect of SV on the optimal boundary price for the put option is greater than that of the call option against the group parameters  $V_2$  or  $V_3$  for the volatility. Moreover, the price sensitivity of the correction term for the put option is drastically larger compared to that for the call option as the volatility decreases.

#### 5. Conclusion

This study examines the approximated formulas of the prices of the perpetual American strangle options with the SVCEV model (PASO-SVCEV) and their free-boundaries, highlighting the features of SV given by Fouque et al. [8]. First, the PDEs for the value of the PASO-SVCEV under the risky asset models were determined, and analytic formulas for the approximated option price for the PASO-SVCEV were obtained using a singular perturbation method. Second, based on the analytical solutions, we demonstrate that our first-approximated solution corresponds to an accurate formula of the PASO-SVCEV, comparing our solution with the Monte Carlo price. Based on the approximation prices, we compared our analytical solutions with the solution derived via the Monte Carlo simulation and demonstrated that it closely corresponds to an accurate formula for the PASO-SVCEV. Third, the numerical experiments revealed the quantitative and qualitative influence of our approximated formulas by analyzing the fast mean-reverting factor embedded in the SV model on the option price and the free-boundary value across various model parameters. This emphasizes that the influence of the SV factor on the option price or the optimal exercise boundary is significant for the effective volatility and the elasticity parameter. Particularly, the impact of the SV factor on the optimal exercise boundary for a put option is more sensitive to the correlation between the risky asset and the volatility or the market price of risk than that on the free boundary for a call option. Finally, the American options or exotic options under diverse models, except for the SV model, are being extensively studied,

even for higher-dimensional model dynamics in financial mathematics. Future studies can extend our selected perpetual American strangle options to a more complicated American option with other types.

#### Acknowledgments

The work of S.-Y. Choi was supported by the National Research Foundation of Korea (NRF), South Korea grant funded by the Korean government (MSIT) (No. RS-2024-00454493). The research by J.-H. Yoon was supported by the National Research Foundation of Korea (NRF), South Korea grant funded by the Korean government (MSIT) (No. 2022R1A5A1033624 and RS-2023-NR076791).

#### Data availability

No data was used for the research described in the article.

#### References

- [1] F. Black, M. Scholes, The pricing of options and corporate liabilities, J. Polit. Econ. 81 (1973) 637-654, http://dx.doi.org/10.1086/260062.
- [2] B. Dupire, Pricing with a smile, Risk 7 (1994) 18-20.
- [3] E. Derman, I. Kani, Riding on a smile, Risk 7 (1994) 32-39.
- [4] J.C. Cox, S.A. Ross, The valuation of options for alternative stochastic processes, J. Financ. Econ. 3 (1976) 145–166, http://dx.doi.org/10.1016/0304-405X(76)90023-4.
- [5] Y. Tian, Z. Zhu, G. Lee, F. Klebaner, K. Hamza, Calibrating and pricing with a stochastic-local volatility model, J. Deriv. 22 (2015) 21–39, http://dx.doi.org/10.3905/jod/2015-22.3.021
- [6] E. Ghysels, A.C. Harvey, E. Renault, 5 stochastic volatility, Handb. Stat. 14 (1996) 119-191, http://dx.doi.org/10.1016/S0169-7161(96)14007-4.
- [7] S.L. Heston, A closed-form solution for options with stochastic volatility with applications to bond and currency options, Rev. Financ. Stud. 6 (1993) 327–343, http://dx.doi.org/10.1093/rfs/6.2.327.
- [8] J.-P. Fouque, G. Papanicolaou, K.R. Sircar, Multiscale Stochastic Volatility for Equity, Interest Rate, and Credit Derivatives, Cambridge University Press,
- [9] J. Hull, A. White, The pricing of options on assets with stochastic volatilities, J. Financ. 42 (1987) 281–300, http://dx.doi.org/10.1111/j.1540-6261.1987.tb02568.x.
- [10] S.Y. Choi, J.P. Fouque, J.H. Kim, Option pricing under hybrid stochastic and local volatility, Quant. Finance 13 (2013) 1157–1165, http://dx.doi.org/10. 1080/14697688.2013.780209.
- [11] D. Kim, S.Y. Choi, J.H. Yoon, Pricing of vulnerable options under hybrid stochastic and local volatility, Chaos Solitons Fractals 146 (2021) 110846, http://dx.doi.org/10.1016/j.chaos.2021.110846.
- [12] J.H. Kim, M.K. Lee, S.Y. Sohn, Investment timing under hybrid stochastic and local volatility, Chaos Solitons Fractals 67 (2014) 58–72, http://dx.doi.org/10.1016/j.chaos.2014.06.007.
- [13] S.Y. Choi, D. Kim, J.H. Yoon, An analytic pricing formula for timer options under constant elasticity of variance with stochastic volatility, AIMS Math. 9 (2024) 2454–2472, http://dx.doi.org/10.3934/math.2024121.
- [14] S.Y. Choi, J.H. Kim, Equity-linked annuities with multiscale hybrid stochastic and local volatility, Scand. Actuar. J. 2016 (2016) 466–487, http://dx.doi.org/10.1080/03461238.2014.955048.
- [15] S.Y. Choi, J.H. Kim, J.H. Yoon, Foreign exchange rate volatility smiles and smirks, Appl. Stoch. Model. Bus. 37 (2021) 628–660, http://dx.doi.org/10. 1002/asmb.2602.
- [16] J. Cao, J.H. Kim, W. Zhang, Pricing variance swaps under hybrid CEV and stochastic volatility, J. Comput. Appl. Math. 386 (2021) 113220, http://dx.doi.org/10.1016/j.cam.2020.113220.
- [17] T.S. Zaevski, American strangle options with arbitrary strikes, J. Futur. Mark. 43 (2023) 880-903, http://dx.doi.org/10.1002/fut.22419.
- [18] J.S. Chaput, L.H. Ederington, Volatility trade design, J. Futur. Mark. 25 (2005) 243-279, http://dx.doi.org/10.1002/fut.20142.
- [19] J.C. Hull, Options Futures and Other Derivatives, Pearson Education India, 2003.
- [20] R. Fahlenbrach, P. Sandås, Does information drive trading in option strategies? J. Bank. Financ. 34 (2010) 2370–2385, http://dx.doi.org/10.1016/j.jbankfin. 2010.02.027.
- [21] C. Kownatzki, B. Putnam, A. Yu, Case study of event risk management with options strangles and straddles, Rev. Financ. Econ. 40 (2022) 150–167, http://dx.doi.org/10.1002/rfe.1143.
- [22] C. Chiarella, A. Ziogas, Evaluation of American strangles, J. Econom. Dynam. Control 29 (2005) 31–62, http://dx.doi.org/10.1016/j.jedc.2003.04.010.
- [23] H.P. McKean Jr., A free boundary problem for the heat equation arising from a problem in mathematical economics, Ind. Manag. Rev. 6 (1965) 32-39.
- [24] F. Moraux, On perpetual American strangles, J. Deriv. 16 (2009) 82-97, http://dx.doi.org/10.3905/jod.2009.16.4.082.
- [25] S. Boyarchenko, Two-point boundary problems and perpetual American strangles in jump-diffusion models, 2006, http://dx.doi.org/10.2139/ssrn.896260, Available at SSRN 896260.
- [26] J. Ma, Y. Zhang, Collocation methods for pricing American strangle options, Differ. Equ. 2 (2012) 2, http://dx.doi.org/10.5539/afr.v1n1p207.
- [27] M. Ha, D. Kim, J.H. Yoon, S.Y. Choi, Pricing for perpetual American strangle options under stochastic volatility with fast mean reversion, Math. Comput. Simulation 227 (2025) 41–57, http://dx.doi.org/10.1016/j.matcom.2024.07.030.
- [28] M.C. Chang, Y.C. Sheu, Free boundary problems and perpetual American strangles, Quant. Finance 13 (2013) 1149–1155, http://dx.doi.org/10.1080/14697688.2013.770159.
- [29] C. Chuang, Valuation of perpetual strangles: A quasi-analytical approach, J. Deriv. 21 (2013) 64-72, http://dx.doi.org/10.3905/jod.2013.21.1.064.
- [30] B. Oksendal, Stochastic Differential Equations: An Introduction with Applications, sixth ed., Springer, 2007.
- [31] L. Tao, The analyticity and general solution of the Cauchy–Stefan problem, Q. J. Mech. Appl. Math. 36 (1983) 487–504, http://dx.doi.org/10.1093/qjmam/36.4.487.
- [32] J.H. Kim, J.H. Yoon, J. Lee, S.Y. Choi, On the stochastic elasticity of variance diffusions, Econ. Model. 51 (2015) 263–268, http://dx.doi.org/10.1016/j.econmod.2015.08.011.
- [33] D. Kim, J. Woo, J.H. Yoon, Pricing American lookback options under a stochastic volatility model, Bull. Korean Math. Soc. 60 (2023) 361–388, http://dx.doi.org/10.4134/BKMS.b220134.